Journal of the Neurological Sciences 331 (2013) 158–160

Contents lists available at SciVerse ScienceDirect

Journal of the Neurological Sciences

journal homepage: www.elsevier.com/locate/jns

Short communication

Exome analysis reveals a Japanese family with spinocerebellar ataxia, autosomal recessive 1

Yaeko Ichikawa [a], Hiroyuki Ishiura [a], Jun Mitsui [a], Yuji Takahashi [a], Shunsuke Kobayashi [b], Hiroshi Takuma [c], Ichiro Kanazawa [d], Koichiro Doi [e], Jun Yoshimura [e], Shinichi Morishita [e], Jun Goto [a], Shoji Tsuji [a,*]

[a] Department of Neurology, Graduate School of Medicine, The University of Tokyo, Japan
[b] Department of Neurology, School of Medicine, Fukushima Medical University, Japan
[c] Department of Neurology, Faculty of Medicine, University of Tsukuba, Japan
[d] International University of Health and Welfare Graduate School, Japan
[e] Department of Computational Biology, Graduate School of Frontier Sciences, The University of Tokyo, Japan

ARTICLE INFO

Article history:
Received 28 December 2012
Received in revised form 17 April 2013
Accepted 13 May 2013
Available online 18 June 2013

Keywords:
Spinocerebellar ataxia
Autosomal recessive 1
Linkage analysis
Exome analysis
Exon capture
Massively parallel sequencing
SETX
Alpha-fetoprotein

ABSTRACT

Spinocerebellar ataxia autosomal recessive 1 (SCAR1/AOA2) is clinically characterized by an early-onset progressive cerebellar ataxia with axonal neuropathy, ocular motor apraxia, and elevation of serum alpha-fetoprotein level. The disorder is caused by mutations in *senataxin* (*SETX*) gene. Here, we report a Japanese SCAR1/AOA2 family with a homozygous nonsense mutation (p.Q1441X) of *SETX* that was identified by exome sequencing. The family was previously reported as early-onset ataxia of undetermined cause. The present study emphasized the role of whole exome-sequence analysis to establish the molecular diagnosis of neurodegenerative disease presenting with diverse clinical presentations.

1. Introduction

Spinocerebellar ataxia, autosomal recessive 1 (SCAR1/AOA2) is an autosomal recessive cerebellar ataxia (ARCA) that is caused by mutations in *senataxin* (*SETX*) [1]. The disorder is characterized clinically by an early-onset progressive cerebellar ataxia, axonal neuropathy, and elevation of serum alpha-fetoprotein (AFP) level [2,3]. We previously reported the case of early-onset ataxia with motor and sensory neuropathy of undetermined cause in a Japanese family [4]. To establish the molecular diagnosis for this family, we applied whole exome-sequence analysis and identified the causative mutation of *SETX*.

2. Patients

Three affected Japanese patients (IV-3, IV-4 and IV-6; Fig. 1A) were reported having early-onset ataxia with motor and sensory neuropathy in the previous study, and they showed normal serum AFP levels [4]. Healthy consanguineous parents and three affected siblings in this family suggest autosomal recessive inheritance. The ages of onset of all the patients were in their teenage years [4].

3. Methods

3.1. Linkage analysis

Genomic DNAs were extracted from peripheral blood leukocytes of the two affected siblings and one unaffected sibling (IV-3, IV-6 and IV-1; Fig. 1A) of the previously reported family after informed consent was obtained [4]. The three members (IV-3, IV-6 and IV-1; Fig. 1A) of the family were genotyped using Genome-Wide Human SNP Array 6.0 (Affymetrix, Santa Clara, CA), and parametric linkage analysis was performed using the pipeline of SNP-HiTLink [5]. The conditions of SNP selection for the linkage analysis were the following; single nucleotide polymorphisms (SNPs) with a p value of >0.001 in the Hardy–Weinberg test, a call rate of >0.98, a confidence score of genotyping <0.2, a minor allele frequency in the controls >0, and intermarker distances of 80 to 120 kb. Parametric multipoint linkage analysis was performed with autosomal recessive model with complete penetrance (disease gene frequency: 0.001) using Allegro version 2 [6].

* Corresponding author at: Department of Neurology, Graduate School of Medicine, The University of Tokyo, 7-3-1 Hongo, Bunkyo-ku, Tokyo 113-8655, Japan. Tel.: +81 3 5800 8972; fax: +81 3 5800 6548.
E-mail address: tsuji@m.u-tokyo.ac.jp (S. Tsuji).

0022-510X/$ – see front matter © 2013 Elsevier B.V. All rights reserved.
http://dx.doi.org/10.1016/j.jns.2013.05.018

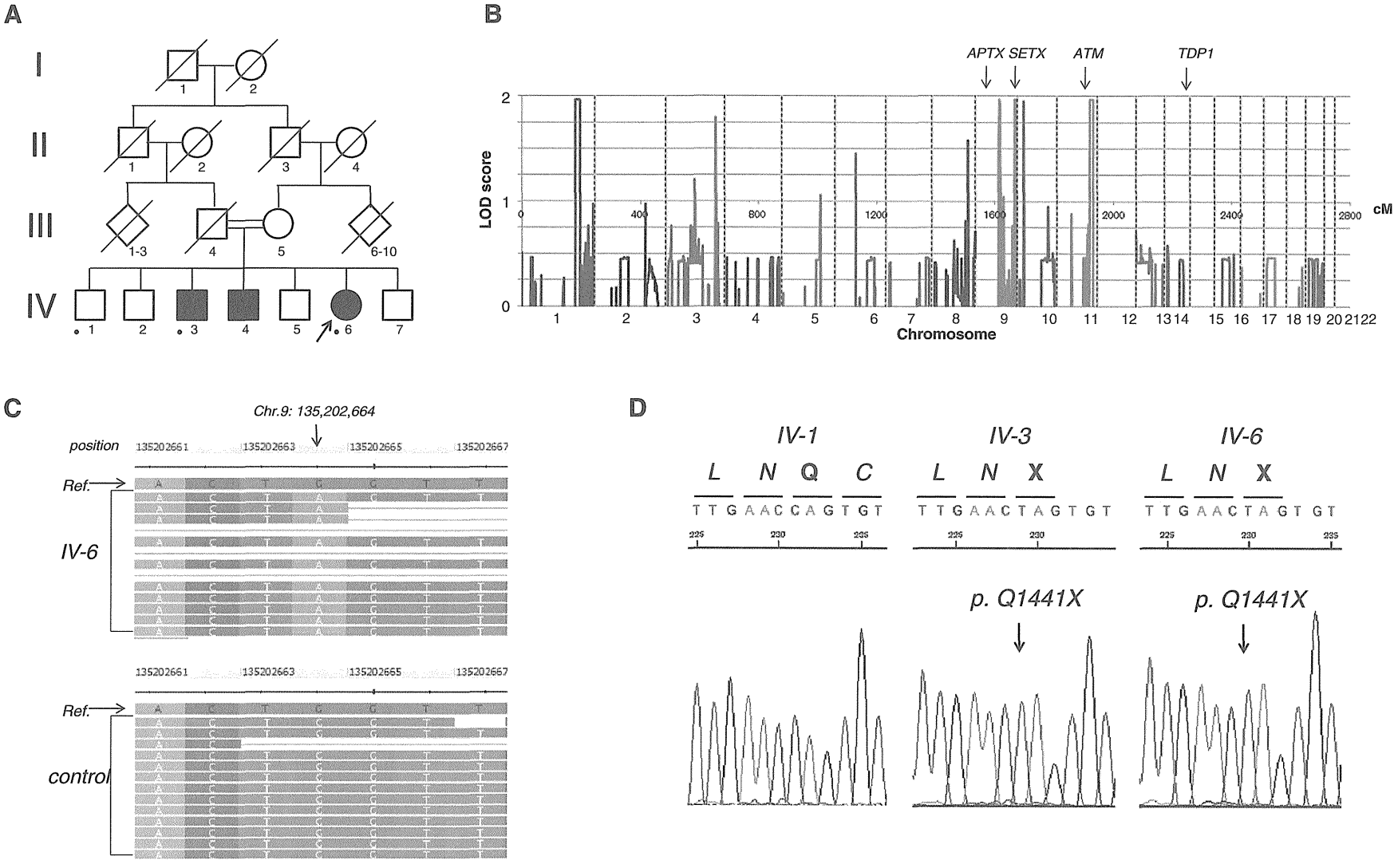

Fig. 1. A. Pedigree of the present family. This chart simplified the pedigree chart of the previous report [4]. Squares and circles indicate males and females, respectively. Diamonds represent males or females. Filled symbols represent affected individuals. A diagonal line through a symbol represents a deceased person. The state of deceased or not is based on the information of the previous report [4] because the family is untraceable now. A person with the arrow is the proband. Persons with available genomic DNAs are indicated by dots. B. Parametric multipoint linkage analysis and candidate regions. Multipoint LOD scores spanning all the chromosomes are shown. The horizontal axis is the cumulative genetic distance (centimorgan: cM) starting at the short arm of chromosome 1. The vertical axis represents LOD scores. Regions on chromosomes 1, 9, 10 and 11 give the highest multipoint LOD score of 1.93. The loci of the causative genes of ARCA with neuropathy are indicated with arrow. The loci of *APTX*, *ATM* and *TDP1* were out of the regions with a multipoint LOD score of 1.93. C. Aligned short reads by exome analysis showed homozygous mutation on position 135,202,664 on chromosome 9. Each short read is represented as a horizontal bar. Ref. means reference sequence (GRCh37/hg19). D. Cosegregated p.Q1441X mutation of *SETX* in this present family [4].

3.2. Exome analysis

The genomic DNA of the proband (IV-6) was captured using TruSeq™ Exome Enrichment Kit (Illumina, San Diego, CA). Massively parallel sequencing was accomplished using GAIIx (110 bp-long paired end read; Illumina). Short reads were aligned to the reference genome (GRCh37/hg19 assembly) with Burrows-Wheeler Alignment tool (BWA) [7], using default parameters. After removing multiple aligned reads (mapping quality of 0) and PCR duplicates, single nucleotide variants (SNVs) and short insertion/deletion variants (indels) were called with SAMtools [8]. After annotation with RefSeq (http://www.ncbi.nlm.nih.gov/RefSeq/), 1000 genomes project database (http://www.1000genomes.org/) and dbSNP135 (http://www.ncbi.nlm.nih.gov/projects/SNP/), all the novel nonsynonymous variant calls were subjected to direct nucleotide sequence analysis for confirmation. We confirmed the mutation in *SETX* by direct nucleotide sequence analysis using a primer pair of SETX 1F: TGAGGCCGACTTACAGAATC and SETX 1R: AGGCAGATCAGACCCAAATC.

4. Results

Multipoint parametric linkage analysis revealed the highest LOD score of 1.93 in five regions on chromosomes 1, 9, 10 and 11, spanning approximately 66 Mb in total including the locus of *SETX* (Fig. 1B). The loci of *APTX*, *ATM* and *TDP1*, the causative genes for ARCAs with neuropathy, were out of the regions with a multipoint LOD score of 1.93 (Fig. 1B).

Massively parallel sequencing analysis was performed using GAIIx, and we obtained 105,741,428 reads. Short reads were aligned to the reference genome sequence (GRCh37/hg19 assembly). Aligned to the reference genome were 87,315,716 reads (82.6%), and 71,469783 reads (67.6%) were aligned uniquely to the target region. The average coverage of the target region was 126.6.

After annotation with RefSeq (http://www.ncbi.nlm.nih.gov/RefSeq/), 1000 genomes project database (http://www.1000genomes.org/) and dbSNP135 (http://www.ncbi.nlm.nih.gov/projects/SNP/), 309 novel nonsynonymous variants were identified, of which six were located in the target regions. Among the six novel nonsynonymous variants, we identified a homozygous mutation of c.4321 C > T (p.Q1441X) of *SETX* cosegregating with the disease in the present family, which was further confirmed by Sanger sequencing (Fig. 1C, D).

5. Discussion

We identified the homozygous p.Q1441X mutation of *SETX* in the family which was previously reported as a family with early-onset ataxia with motor and sensory neuropathy of undetermined cause in 2007 [4]. The homozygous p.Q1441X mutation in *SETX* was previously reported in an unrelated Japanese family [1,2], thus confirming the diagnosis of SCAR1/AOA2 in our family. The finding was unexpected, because the diagnosis of SCAR1/AOA2 was previously considered unlikely on the basis of normal serum AFP levels at that time [4]. The stocked serum of the proband's affected brother (IV-3; Fig. 1A) was available and serum AFP level was measured, which revealed a moderately elevated serum AFP level (33.2 ng/ml, normal value < 9 ng/ml), further confirming the diagnosis of SCAR1/AOA2.

The clinical feature of SCAR1/AOA2 was characterized by early onset progressive ataxia with neuropathy [2]. Previous studies revealed polyneuropathy in 97.5% of SCAR1/AOA2 patients, cerebellar atrophy in 96%, occasional oculomotor apraxia (OMA) in 51%, and elevated serum AFP levels in 99%, [3]. Given the elevated serum AFP level, our patients showed rather typical clinical presentations as SCAR1/AOA2. Since the previous medical records were discarded, we could not confirm the exact values of AFP, making it difficult to interpret the serum AFP levels in our previous reports. Nonetheless, the increased serum AFP level obtained from the analysis of the stocked serum of the proband's affected brother (IV-3; Fig. 1A) further confirmed the diagnosis of SCAR1/AOA2.

ARCA is a heterogeneous group of neurodegenerative diseases that are clinically characterized by progressive ataxia in association with various neurological and/or biochemical findings and more than 15 causative genes for ARCA have been identified [9], making the prioritization of genes for molecular diagnosis difficult. Availability of exome analysis and massively parallel sequencing technology are expected to accelerate the comprehensive mutational analyses to establish the molecular diagnosis of diseases associated with numerous causative genes, as demonstrated in this report.

Conflict of interest

The authors declare that they have no conflict of interest.

Acknowledgment

This work was supported in part by KAKENHI (Grant-in-Aid for Scientific Research) on Scientific Research on Innovative Areas (Exploring Molecular Basis for Brain Diseases Based on Personal Genomics) and a grant from the Research Committee for Ataxic Diseases, Ministry of Health, Labor, and Welfare, Japan.

References

[1] Moreira MC, Klur S, Watanabe M, Nemeth AH, Le Ber I, Moniz JC, et al. Senataxin, the ortholog of a yeast RNA helicase, is mutant in ataxia–ocular apraxia 2. Nat Genet 2004;36:225–7.
[2] Watanabe M, Sugai Y, Concannon P, Koenig M, Schmitt M, Sato M, et al. Familial spinocerebellar ataxia with cerebellar atrophy, peripheral neuropathy, and elevated level of serum creatine kinase, gamma-globulin, and alpha-fetoprotein. Ann Neurol 1998;44:265–9.
[3] Anheim M, Monga B, Fleury M, Charles P, Barbot C, Salih M, et al. Ataxia with oculomotor apraxia type 2: clinical, biological and genotype/phenotype correlation study of a cohort of 90 patients. Brain 2009;132:2688–98.
[4] Kobayashi S, Takuma H, Murayama S, Sakurai M, Kanazawa IA. Japanese family with early-onset ataxia with motor and sensory neuropathy. J Neurol Sci 2007;254:44–8.
[5] Fukuda Y, Nakahara Y, Date H, Takahashi Y, Goto J, Miyashita A, et al. SNP HiTLink: a high-throughput linkage analysis system employing dense SNP data. BMC Bioinforma 2009;10:121.
[6] Gudbjartsson DF, Thorvaldsson T, Kong A, Gunnarsson G, Ingolfsdottir A. Allegro version 2. Nat Genet 2005;37:1015–6.
[7] Li H, Durbin R. Fast and accurate short read alignment with Burrows–Wheeler transform. Bioinformatics 2009;25:1754–60.
[8] Li H, Handsaker B, Wysoker A, Fennell T, Ruan J, Homer N, et al. The sequence alignment/map format and SAMtools. Bioinformatics 2009;25:2078–9.
[9] Fogel BL, Perlman S. Clinical features and molecular genetics of autosomal recessive cerebellar ataxias. Lancet Neurol 2007;6:245–57.

RESEARCH ARTICLE

AMERICAN JOURNAL OF medical genetics PART B
Neuropsychiatric Genetics

CSF1R Mutations Identified in Three Families With Autosomal Dominantly Inherited Leukoencephalopathy

Jun Mitsui,[1] Takashi Matsukawa,[1] Hiroyuki Ishiura,[1] Koichiro Higasa,[2] Jun Yoshimura,[2] Taro L. Saito,[2] Budrul Ahsan,[1] Yuji Takahashi,[1] Jun Goto,[1] Atsushi Iwata,[1,3] Yuki Niimi,[4] Yuuichi Riku,[4] Yoji Goto,[4] Kazuo Mano,[4] Mari Yoshida,[5] Shinichi Morishita,[2] and Shoji Tsuji[1,6,7]*

[1]Department of Neurology, Graduate School of Medicine, The University of Tokyo, Tokyo, Japan

[2]Department of Computational Biology, Graduate School of Frontier Sciences, The University of Tokyo, Chiba, Japan

[3]Department of Molecular Neuroscience on Neurodegeneration, The University of Tokyo, Tokyo, Japan

[4]Department of Neurology, Nagoya Daiichi Red Cross Hospital, Aichi, Japan

[5]Department of Neuropathology, Institute for Medical Science of Aging, Aichi Medical University, Aichi, Japan

[6]Medical Genome Center, Graduate School of Medicine, The University of Tokyo, Tokyo, Japan

[7]Division of Applied Genetics, National Institute of Genetics, Shizuoka, Japan

Manuscript Received: 24 April 2012; Manuscript Accepted: 6 September 2012

Genetic and phenotypic heterogeneities are considerably high in adult-onset leukoencephalopathy, in which comprehensive mutational analyses of the candidate genes by conventional methods are too laborious. We applied exome sequencing to conduct a comprehensive mutational analysis of genes for autosomal dominant leukoencephalopathies. Genomic DNA samples from four patients of three families with autosomal dominantly inherited adult-onset leukodystrophy were subjected to exome sequencing. On the basis of the results, 21 patients with adult-onset sporadic leukodystrophy and one patient with pathologically proven HDLS were additionally screened for *CSF1R* mutations. Exome sequencing identified heterozygous *CSF1R* mutations (p.I794T and p.R777W) in two families. I794T has recently been reported as a causative mutation for hereditary diffuse leukoencephalopathy with spheroids (HDLS), and R777W is a novel mutation. Although mutational analysis of *CSF1R* in 21 sporadic cases revealed no mutations, another novel *CSF1R* mutation, p.C653Y, was identified in one patient with autopsy-proven HDSL. These variants were located in the PTK domain where the causative mutations cluster. Functional prediction of the mutant *CSF1R* as well as cross-species conservation of the affected amino acids supports the notion that these variants are pathogenic for HDLS. Exome sequencing is useful for a comprehensive mutational analysis of causative genes for hereditary leukoencephalopathies, and *CSF1R* should be considered a candidate gene for patients with autosomal dominant leukoencephalopathies. © 2012 Wiley Periodicals, Inc.

Key words: hereditary diffuse leukoencephalopathy with spheroids; *CSF1R*; exome sequencing; molecular diagnosis

How to Cite this Article:
Mitsui J, Matsukawa T, Ishiura H, Higasa K, Yoshimura J, Saito TL, Ahsan B, Takahashi Y, Goto J, Iwata A, Niimi Y, Riku Y, Goto Y, Mano K, Yoshida M, Morishita S, Tsuji S. 2012. *CSF1R* Mutations Identified in Three Families With Autosomal Dominantly Inherited Leukoencephalopathy.
Am J Med Genet Part B.

INTRODUCTION

Hereditary diffuse leukoencephalopathy with spheroids (HDLS) is a rare autosomal dominant disease characterized neuropatholog-

Additional supporting information may be found in the online version of this article.

Jun Mitsui and Takashi Matsukawa equally contributed to this work.
Grant sponsor: KAKENHI; Grant numbers: 22129001, 22129002; Grant sponsor: Ministry of Education, Culture, Sports, Science, and Technology of Japan; Grant sponsor: Ministry of Health, Welfare and Labour, Japan.

*Correspondence to:
Shoji Tsuji, Ph.D., M.D., Department of Neurology, Graduate School of Medicine, The University of Tokyo, 7-3-1 Hongo, Bunkyo-ku, Tokyo 113-8655, Japan. E-mail: tsuji@m.u-tokyo.ac.jp

Article first published online in Wiley Online Library (wileyonlinelibrary.com): 00 Month 2012
DOI 10.1002/ajmg.b.32100

ically by myelin loss and the presence of axonal spheroids. The clinical presentations of HDLS are characterized by a mean age at onset of 39 ± 15 years (range: 8–78 years) and insidiously progressive behavioral, cognitive, and/or motor dysfunctions (parkinsonism, ataxia, pyramidal dysfunctions, and epilepsy) [Axelsson et al., 1984; Wider et al., 2009]. White matter abnormalities are predominantly found in the frontal and parietal lobes accompanied by evolving cortical atrophy on magnetic resonance imaging (MRI). Because neither the clinical symptoms nor the MRI findings are specific, until recently, diagnosis of HDLS has depended solely on histopathological examination [Axelsson et al., 1984] or brain biopsy [Mateen et al., 2010]. The causative gene for HDLS has recently been identified to be the colony stimulating factor 1 receptor gene (*CSF1R*) [Rademakers et al., 2011].

Leukoencephalopathies are clinically and genetically heterogeneous diseases and a number of diseases need to be considered for the differential diagnosis. The following are among the leukoencephalopathies with autosomal dominant inheritance: cerebral autosomal dominant arteriopathy with subcortical infarcts and leukoencephalopathy (CADASIL) [Joutel et al., 1996], lamin B1 duplications [Padiath et al., 2006], Alexander disease [Brenner et al., 2001], several types of cerebral amyloid angiopathy and small vessel diseases [Ghiso et al., 1986; Levy et al., 1990; Van Broeckhoven et al., 1990; Sherrington et al., 1995; Vidal et al., 1999; Paloneva et al., 2000; Brenner et al., 2001; Gould et al., 2006; Padiath et al., 2006; Richards et al., 2007], and HDLS. The following are among the leukoencephalopathies with autosomal recessive inheritance: cerebral autosomal recessive arteriopathy with subcortical infarcts and leukoencephalopathy (CARASIL) [Hara et al., 2009], vanishing white matter disease [Leegwater et al., 2001; van der Knaap et al., 2002], Nasu-Hakola disease [Paloneva et al., 2000; Kondo et al., 2002], Krabbe disease [Sakai et al., 1994], and metachromatic leukodystrophy [Polten et al., 1991]. Hence, establishing the diagnosis of these conditions is often difficult in clinical practice, necessitating comprehensive mutational analysis of a substantial number of causative genes for leukoencephalopathies [Köhler, 2010]. Here, we applied exome sequencing employing massively parallel sequencers for a comprehensive mutational analysis of causative genes for leukoencephalopathies, and identified cases with mutations in *CSF1R*.

METHODS

Exome Sequencing Analysis

Written informed consent was obtained from all the participants. Genomic DNA samples were extracted from peripheral blood leukocytes following standard procedures. We conducted exome sequencing in four individuals of three Japanese families with autosomal dominantly inherited adult-onset leukodystrophy of unknown etiology (II-6 and III-1 of Family 1; III-3 of Family 2; and III-1 of Family 3, Fig. 1A). Exonic sequences were enriched using a TruSeq Exome Enrichment kit (Illumina, San Diego, CA) and subjected to massively parallel sequence analysis employing an Illumina Genome Analyzer IIx platform (Illumina) following the manufacturer's instructions. Burrows Wheeler Aligner [Li and Durbin, 2009] and Samtools [Li et al., 2009] were used with the default settings for alignment of raw reads and variation detection. All the genomic variants were filtered against dbSNP (build 135) [http://www.ncbi.nlm.nih.gov/snp]. Aligned short reads were viewed using the University of Tokyo Genome Browser (UTGB) [Saito et al., 2009]. Variant confirmations were conducted by direct nucleotide sequence analysis using an ABI 3100 Genetic Analyzer (Life Technologies, Foster City, CA).

Screening for *CSF1R* Mutations in Patients With Sporadic Leukoencephalopathy and in a Case of Pathologically Diagnosed HDSL

To investigate the frequency of *CSF1R* mutations in patients with sporadic leukoencephalopathies, we further conducted the direct nucleotide sequence analysis of *CSF1R* in 21 Japanese patients with the clinical diagnosis of sporadic leukoencephalopathies. Because all the previously reported mutations in patients with HDLS are solely located in the protein tyrosine kinase (PTK) domain of CSF1R, we screened for mutations of *CSF1R* exons 12–20. In addition, the result of mutational analysis of *CSF1R* for one pathologically proven case of HDLS (III-1 of Family 4, Fig. 1A) was also included in this study.

In Silico Analyses

To predict the impact of amino acid substitutions on protein activity, we conducted a battery of in silico analyses using Polymorphism phenotyping v2 (Polyphen-2) [Adzhubei et al., 2010]; SIFT [Ng and Henikoff, 2001]; MutationTaster [Schwarz et al., 2010]; and MUPro [Cheng et al., 2006], along with species conservation analysis using UCSC Genome Browser [Karolchik et al., 2007].

RESULTS

Exome Sequencing

We obtained mean coverage depths of 109.4, 100.1, 137.7, and 195.0 in II-6 and III-1 of Family 1, III-3 of Family 2, and III-1 of Family 3, respectively, which are sufficient for examining the exons for mutations. All the nonsynonymous and splice-site single-nucleotide variants (SNVs), or insertions and deletions in coding sequences (coding indels), which were not registered in dbSNP135, were obtained (hereafter collectively called "novel variants"). The results of the exome sequence analysis are summarized in Table I. We then screened for variants involving previously known causative genes of autosomal dominant adult-onset leukoencephalopathies (*NOTCH3*, *LMNB1*, *GFAP*, *APP*, *PSEN1*, *PSEN2*, *CST3*, *ITM2B*, *TREX1*, *COL4A1*, and *CSF1R*). We solely found a heterozygous p.I794T mutation in *CSF1R* that was shared among the affected individuals (III-1 and II-6) of Family 1 (Table II). This mutation is identical to that previously identified as the causative mutation for HDLS [Rademakers et al., 2011]. We, furthermore, identified a novel *CSF1R* mutation (p.R777W) in III-3 of Family 2 (Fig. 2). There were no other novel variants in the known causative genes either in Family 1 or in Family 2 (Table II). No candidate variants were identified in the known causative genes for autosomal dominant leukoencephalopathies in III-1 of Family 3.

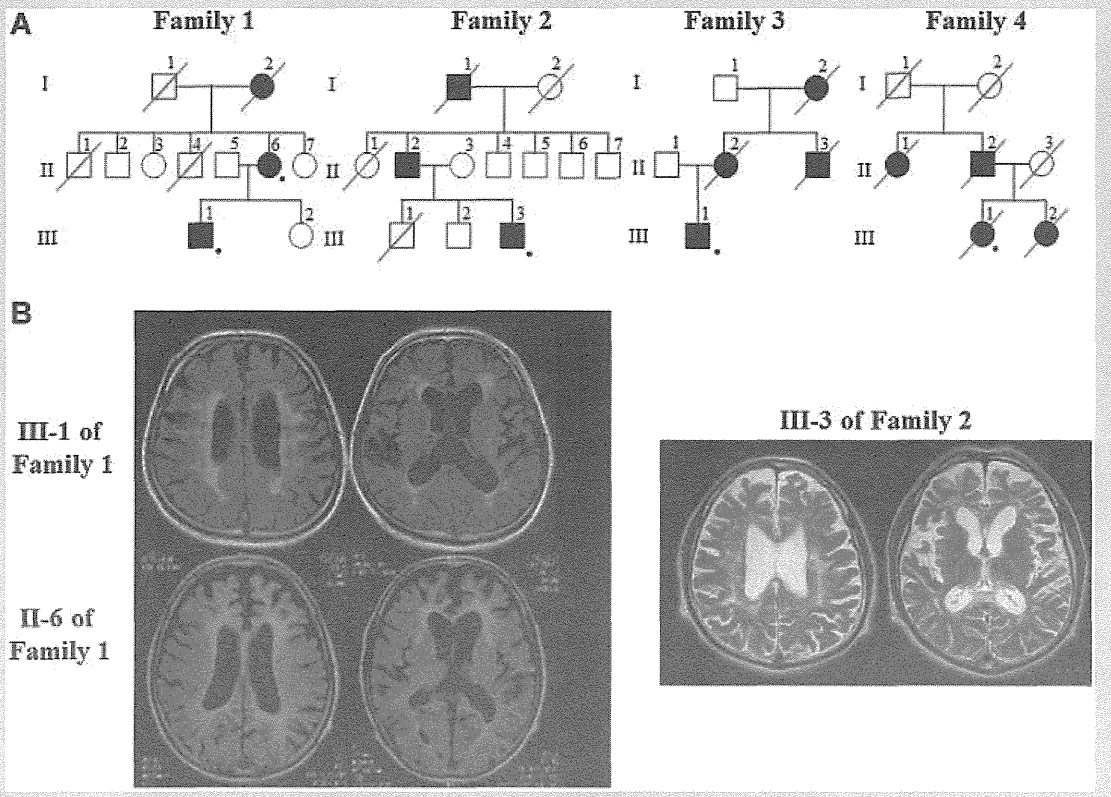

FIG. 1. Pedigree charts and neuroimaging findings. A: Males, squares; female, circles; affected individuals, solid symbols; unaffected individuals, open symbols; available genomic DNAs, dot. B: Axial fluid attenuated inversion recovery (FLAIR) magnetic resonance images of individual III-1 of Family 1 at the age of 54 and those of individual II-6 of Family 1 at the age of 70, showing atrophy in frontal, parietal, and medial temporal lobes, with periventricular confluent hyperintensities. Axial T2-weighted magnetic resonance images of individual III-3 of Family 2 at the age of 41, showing atrophy in frontal, parietal and temporal lobes, with confluent hyperintensities in periventricular regions including corpus callosum.

Screening for *CSF1R* Mutations in Patients With Sporadic Leukoencephalopathy and in a Patient With Pathologically Diagnosed HDSL

Considering the possibilities of reduced penetrance, insufficient information on the family history, or de novo mutations in *CSF1R* in patients with sporadic leukoencephalopathies, we investigated the frequencies of *CSF1R* mutations in 21 patients with adult-onset sporadic leukoencephalopathy. In this sporadic case series, however, no mutations were identified. We further screened for *CSF1R* mutations in a patient with pathologically diagnosed HDLS (III-1 of Family 4, Fig. 1), which revealed another novel *CSF1R* mutation (p.C653Y).

Implications of Mutant *CSF1R* as Cause of HDSL

None of the identified variants (C653Y, R777W, and I794T) were identified either in dbSNP135, 1,000 Genomes (http://

TABLE I. Summary of Exome Sequence Analysis Results

Family	Individual	Read	Mapped read	Coverage	Proportion of target bases covered > 10-fold read depth (%)	SNVs (total)	Unknown NS/SS SNVs	Indels (total)	Unknown coding indels
1	II-6	67.2 M	61.8 M (91.8%)	109.4	89.1	227,491	354	20,965	32
	III-1	61.4 M	56.5 M (92.0%)	100.1	88.2	218,020	349	20,261	30
2	III-3	77.9 M	64.9 M (83.4%)	137.7	80.8	193,528	396	18,271	36
3	III-1	94.4 M	91.9 M (97.5%)	195.0	80.8	253,999	292	24,951	31

SNVs, single nucleotide variants; NS, nonsynonymous; SS, splice-site.

TABLE II. Nonsynonymous Variants in Known Causative Genes of Autosomal Dominant Adult-Onset Leukoencephalopathies (*NOTCH3, LMNB1, GFAP, APP, PSEN1, PSEN2, CST3, ITM2B, TREX1, COL4A1*, and *CSF1R*)

Family	Individual	Variants registered in dbSBP135	Novel variants (not registered in dbSNP135)
1	II-6	*CSF1R*, rs10079250	*CSF1R*, I794T
		NOTCH3, rs1044009	
		COL4A1, rs536174	
		COL4A1, rs9515185	
	III-1	*CSF1R*, rs10079250	*CSF1R*, I794T
		NOTCH3, rs1044009	
		COL4A1, rs3742207	
		COL4A1, rs536174	
2	III-3	*NOTCH3*, rs1044009	*CSF1R*, R777W
		COL4A1, rs3742207	
		COL4A1, rs536174	
3	III-1	*NOTCH3*, rs1044009	None
		COL4A1, rs536174	

www.1000genomes.org/, accessed at June 2012), NHLBI Exome Sequencing Project (http://evs.gs.washington.edu/EVS/, EVS-v0.0.13), or 720 samples (individuals with other neurological diseases from the Japanese population) of inhouse exome database, showing that these are novel variants irrespective of ethnicity. In the above databases, many rare and relatively common missense variants are registered, many of which map near the two newly identified variants. Nonetheless, the absence of the two newly identified variants in these databases is strongly indicative of pathogenicity. As the family members were unavailable for segregation analyses of the mutation except for Family 1, we then investigated cross-species conservation of the mutated amino acids and functional prediction analyses to obtain supporting evidence for the pathogenicity of the mutant CSF1R identified in this study. As shown in Figure 3B, a strong conservation of the affected amino acids across species was well demonstrated for all three variants. In silico functional prediction analyses unanimously predicted all the identified variants to be "Probably damaging" by Polyphen-2, "Damaging" by SIFT, "Disease-causing" by MutationTaster, and "Stability decreasing" by MUPro (Fig. 3C). Intriguingly, they were all located in the PTK domain similarly to previously reported mutations (Fig. 3A). Taken together, we considered that all the identified variants (one known causative mutation and two novel mutations) were pathogenic for HDLS.

Clinical Features

In total, three families with adult-onset leukoencephalopathy with *CSF1R* mutations were identified, including one family with the pathological diagnosis of HDSL. Detailed clinical information was available for six individuals from the three families. A summary of the clinical characteristics is shown in Table III. The mean age at onset of the six patients was 51.0 ± 10.0 years (range: 38–65 years), and the mean age at death of the three deceased patients was 55.7 ± 10.2 years (range: 44–63 years). Initial symptoms substantially varied within and across the families. Notably, the proband (III-3) of Family 2 developed alcoholism 4 years before his admission to our hospital, and substance abuse such as alcoholism has often been reported in HDLS [Axelsson et al., 1984; van der Knaap et al., 2000]. In the course of disease development, personality and behavioral changes, and dementia were highly prevalent. Parkinsonism was observed in one of the three patients, and seizures were present in two of the five patients. Brain MR images of individuals III-1 and II-6 of Family 1, and III-3 of Family 2 are shown in Figure 1B, which showed atrophy in the frontal, parietal, and medial temporal lobes, with periventricular confluent hyperintensities on fluid attenuated inversion recovery (FLAIR) or T2-weighted images. Detailed information on the medical history of the patients is provided in Supplementary Text.

DISCUSSION

Various mutations in *CSF1R* have been described in 15 families with HDLS [Rademakers et al., 2011; Kinoshita et al., 2012], and all the causative mutations are located in the PTK domain of CSF1R (Fig. 3A). We herein identified *CSF1R* mutations in three families with autosomal dominantly inherited leukoencephalopathy (two with leukoencephalopathy of unknown etiology and one with autopsy-proven HDLS). The I794T mutation is the same as that identified in a previously reported family in the United States (Family SC) [Van Gerpen et al., 2008], and the novel mutations identified (C653Y and R777W) are also located at the PTK domain. Taken together with strong conservation of the affected amino acids across species (Fig. 3B), and in silico prediction of functional impairment associated with the mutations (Fig. 3C), all the identified mutations in this study are considered to be pathogenic.

HDLS is indeed a rare hereditary disease, and it is likely unrecognized owing to the nonspecific MRI findings, which are common to ischemic changes or other causes of white matter diseases, and also owing to the quite variable clinical presentations. The affected individuals (III-1 and II-6) of Family 1 started to show cognitive impairments in their fifth or sixth decades, which relatively rapidly worsened year by year, and their clinical diagnosis was atypical Alzheimer disease. The examined member (III-3) of Family 2

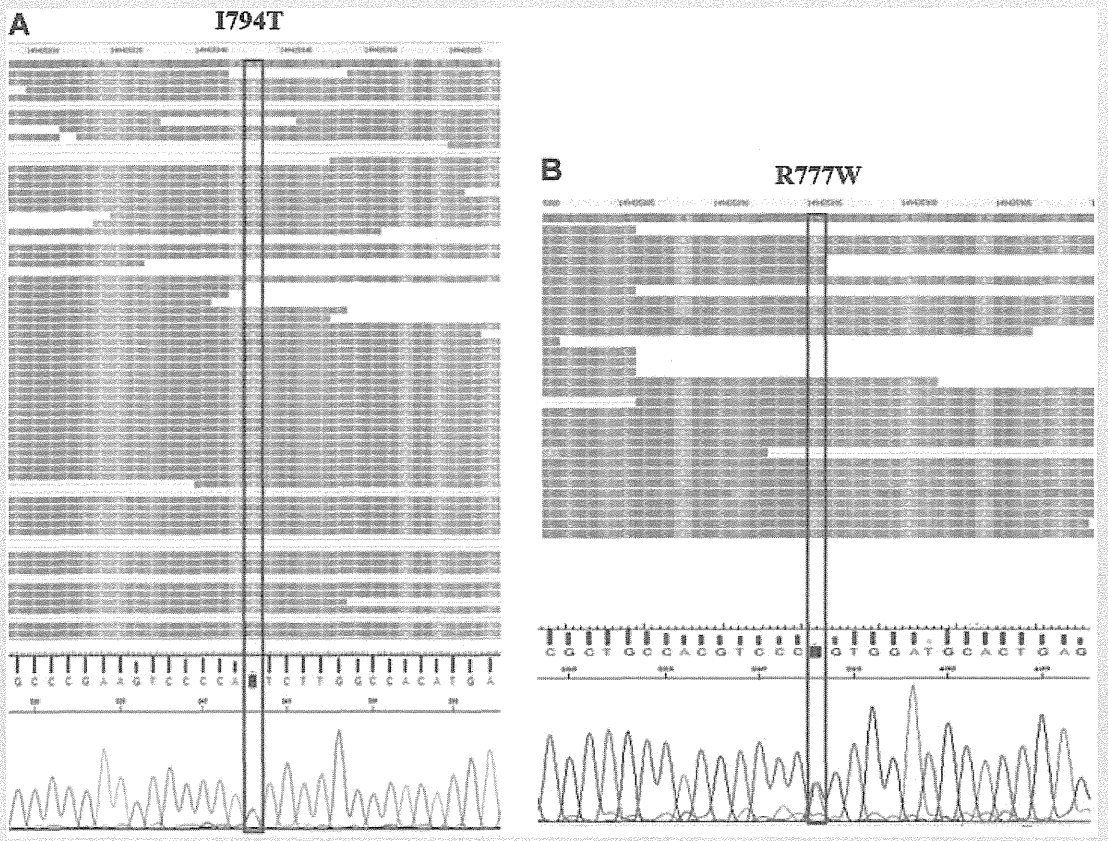

FIG. 2. Identification of causative mutation in *CSF1R*. Aligned short reads and the corresponding electropherograms of direct nucleotide sequence analysis are shown (A: I794T mutation; B: R777W mutation).

gradually developed alcoholism in his late thirties, and around the age of 40, his cognitive impairment and gait disturbance worsened rapidly. His clinical diagnosis was cerebral small vascular disease with unknown etiology. It should be emphasized that the affected individuals in Families 1 and 2 did not have a diagnosis of HDLS at the outset, and that only through exome sequencing was *CSF1R* identified. Thus *CSF1R* should be considered a candidate gene for autosomal dominant leukoencephalopathies regardless of whether biopsy has been obtained to look for spheroids. To data, the diagnosis of HDLS has been made solely by neuropathological

TABLE III. Clinical Characteristics of Six Individuals From Three Japanese Families With *CSF1R* Mutations

							Clinical features during course of disease development				
Family	Individual	*CSF1R* mutation	Sex	Onset age	Death age	Initial symptom	Personality and behavioral changes	Dementia	Depression	Parkinsonism	Seizures
1	II-6	I794T	Female	60	Alive	Forgetfulness	+	+	−	−	−
	III-1	I794T	Male	52	60	Apathy	+	+	+	+	−
2	II-2	Not tested	Male	65	Alive	Depression	+	+	Not described	Not described	+
	III-3	R777W	Male	38	Alive	Alcoholism	+	+	+	−	−
4	III-1	C653Y	Female	48	63	Repetitive behavior	+	+	Not described	Not described	+
	III-2	Not tested	Female	43	44	Body weight loss	Not described	Not described	Not described	Not described	Not described

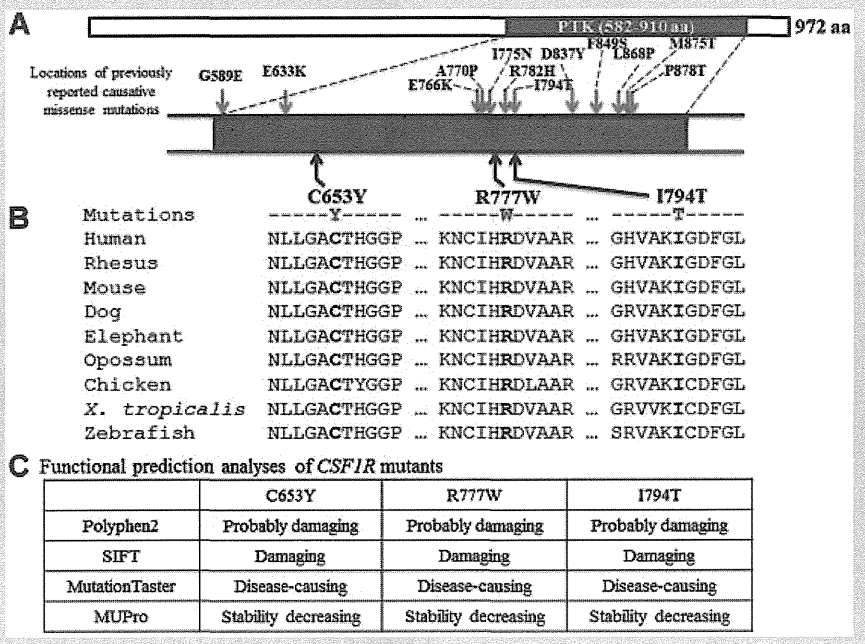

C Functional prediction analyses of *CSF1R* mutants

	C653Y	R777W	I794T
Polyphen2	Probably damaging	Probably damaging	Probably damaging
SIFT	Damaging	Damaging	Damaging
MutationTaster	Disease-causing	Disease-causing	Disease-causing
MUPro	Stability decreasing	Stability decreasing	Stability decreasing

FIG. 3. Protein domain structure of CSF1R with summary of *CSF1R* mutations. A: Location of protein tyrosine kinase domain (PTK) of CSF1R, with summary of mutations identified in the present study as well as previously reported causative missense mutations [Rademakers et al., 2011; Kinoshita et al., 2012]. B: Comparative genomic analysis of multiple species for the parts of the PTK domain where the mutations occur is shown. C: Summary of in silico analyses of pathogenicity prediction (Polyphen-2, SIFT, MutationTaster, and MUPro).

findings. With the availability of mutational analysis of *CSF1R*, the clinical spectrum of patients with *CSF1R* mutations and genotype–phenotype correlations should be thoroughly investigated.

There are numerous genes related to leukoencephalopathies, for which it is difficult to focus on particular genes for the mutational analysis depending solely on phenotypes. Targeted sequencing would be as effective as exome sequencing and certainly a lot less expensive currently. On the other hand, a growing number of causative genes have been identified in Mendelian diseases, and comprehensive mutational analysis of causative genes may necessitate updating of a method for target sequencing on a continuous basis, which is often difficult in clinical practice. Considering this situation, exome sequencing has become a common method of molecular diagnosis of Mendelian diseases. On the other hand, we are encountering an increasing number of very rare variants that are not necessarily pathogenic. Because exome sequencing provides virtually all the variants of genes that are relevant to a particular disease group, that is, leukoencephalopathies in this study, knowledge of allele frequencies of variants in a specific phenotyped population is indeed quite helpful for interpreting which of those variants are likely to be pathogenic.

ACKNOWLEDGMENTS

This work was supported in part by KAKENHI (Grants-in-Aid for Scientific Research on Innovative Areas (22129001 and 22129002) and the Global COE Program from the Ministry of Education, Culture, Sports, Science, and Technology of Japan, and a Grant-in-Aid (H23-Jitsuyoka (Nanbyo)-Ippan-004) from the Ministry of Health, Welfare and Labour, Japan.

REFERENCES

Adzhubei IA, Schmidt S, Peshkin L, Ramensky VE, Gerasimova A, Bork P, Kondrashov AS, Sunyaev SR. 2010. A method and server for predicting damaging missense mutations. Nat Methods 7(4):248–249.

Axelsson R, Röyttä M, Sourander P, Akesson HO, Andersen O. 1984. Hereditary diffuse leucoencephalopathy with spheroids. Acta Psychiatr Scand Suppl 314:1–65.

Brenner M, Johnson AB, Boespflug-Tanguy O, Rodriguez D, Goldman JE, Messing A. 2001. Mutations in GFAP, encoding glial fibrillary acidic protein, are associated with Alexander disease. Nat Genet 27(1):117–120.

Cheng J, Randall A, Baldi P. 2006. Prediction of protein stability changes for single-site mutations using support vector machines. Proteins 62(4): 1125–1132.

Ghiso J, Jensson O, Frangione B. 1986. Amyloid fibrils in hereditary cerebral hemorrhage with amyloidosis of Icelandic type is a variant of gamma-trace basic protein (cystatin C). Proc Natl Acad Sci USA 83(9):2974–2978.

Gould DB, Phalan FC, van Mil SE, Sundberg JP, Vahedi K, Massin P, Bousser MG, Heutink P, Miner JH, Tournier-Lasserve E, John SW. 2006. Role of COL4A1 in small-vessel disease and hemorrhagic stroke. N Engl J Med 354(14):1489–1496.

Hara K, Shiga A, Fukutake T, Nozaki H, Miyashita A, Yokoseki A, Kawata H, Koyama A, Arima K, Takahashi T, Ikeda M, Shiota H, Tamura M, Shimoe Y, Hirayama M, Arisato T, Yanagawa S, Tanaka A, Nakano I, Ikeda S, Yoshida Y, Yamamoto T, Ikeuchi T, Kuwano R, Nishizawa M,

Tsuji S, Onodera O. 2009. Association of HTRA1 mutations and familial ischemic cerebral small-vessel disease. N Engl J Med 360(17):1729–1739.

Joutel A, Corpechot C, Ducros A, Vahedi K, Chabriat H, Mouton P, Alamowitch S, Domenga V, Cécillion M, Marechal E, Maciazek J, Vayssiere C, Cruaud C, Cabanis EA, Ruchoux MM, Weissenbach J, Bach JF, Bousser MG, Tournier-Lasserve E. 1996. Notch3 mutations in CADASIL, a hereditary adult-onset condition causing stroke and dementia. Nature 383(6602):707–710.

Karolchik D, Bejerano G, Hinrichs AS, Kuhn RM, Miller W, Rosenbloom KR, Zweig AS, Haussler D, Kent WJ. 2007. Comparative genomic analysis using the UCSC genome browser. Methods Mol Biol 395:17–34.

Kinoshita M, Yoshida K, Oyanagi K, Hashimoto T, Ikeda S. 2012. Hereditary diffuse leukoencephalopathy with axonal spheroids caused by R782H mutation in CSF1R: Case report. J Neurol Sci 318(1–2):115–118.

Köhler W. 2010. Leukodystrophies with late disease onset: An update. Curr Opin Neurol 23(3):234–241.

Kondo T, Takahashi K, Kohara N, Takahashi Y, Hayashi S, Takahashi H, Matsuo H, Yamazaki M, Inoue K, Miyamoto K, Yamamura T. 2002. Heterogeneity of presenile dementia with bone cysts (Nasu–Hakola disease): Three genetic forms. Neurology 59(7):1105–1107.

Leegwater PA, Vermeulen G, Könst AA, Naidu S, Mulders J, Visser A, Kersbergen P, Mobach D, Fonds D, van Berkel CG, Lemmers RJ, Frants RR, Oudejans CB, Schutgens RB, Pronk JC, van der Knaap MS. 2001. Subunits of the translation initiation factor eIF2B are mutant in leukoencephalopathy with vanishing white matter. Nat Genet 29(4):383–388.

Levy E, Carman MD, Fernandez-Madrid IJ, Power MD, Lieberburg I, van Duinen SG, Bots GT, Luyendijk W, Frangione B. 1990. Mutation of the Alzheimer's disease amyloid gene in hereditary cerebral hemorrhage, Dutch type. Science 248(4959):1124–1126.

Li H, Durbin R. 2009. Fast and accurate short read alignment with Burrows–Wheeler transform. Bioinformatics 25(14):1754–1760.

Li H, Handsaker B, Wysoker A, Fennell T, Ruan J, Homer N, Marth G, Abecasis G, Durbin R. 2009. The sequence alignment/map format and SAM tools. Bioinformatics 25(16):2078–2079.

Mateen FJ, Keegan BM, Krecke K, Parisi JE, Trenerry MR, Pittock SJ. 2010. Sporadic leucodystrophy with neuroaxonal spheroids: Persistence of DWI changes and neurocognitive profiles: A case study. J Neurol Neurosurg Psychiatry 81(6):619–622.

Ng PC, Henikoff S. 2001. Predicting deleterious amino acid substitutions. Genome Res 11(5):863–874.

Padiath QS, Saigoh K, Schiffmann R, Asahara H, Yamada T, Koeppen A, Hogan K, Ptácek LJ, Fu YH. 2006. Lamin B1 duplications cause autosomal dominant leukodystrophy. Nat Genet 38(10):1114–1123.

Paloneva J, Kestilä M, Wu J, Salminen A, Böhling T, Ruotsalainen V, Hakola P, Bakker AB, Phillips JH, Pekkarinen P, Lanier LL, Timonen T, Peltonen L. 2000. Loss-of-function mutations in TYROBP (DAP12) result in a presenile dementia with bone cysts. Nat Genet 25(3):357–361.

Polten A, Fluharty AL, Fluharty CB, Kappler J, von Figura K, Gieselmann V. 1991. Molecular basis of different forms of metachromatic leukodystrophy. N Engl J Med 324(1):18–22.

Rademakers R, Baker M, Nicholson AM, Rutherford NJ, Finch N, Soto-Ortolaza A, Lash J, Wider C, Wojtas A, DeJesus-Hernandez M, Adamson J, Kouri N, Sundal C, Shuster EA, Aasly J, MacKenzie J, Roeber S, Kretzschmar HA, Boeve BF, Knopman DS, Petersen RC, Cairns NJ, Ghetti B, Spina S, Garbern J, Tselis AC, Uitti R, Das P, Van Gerpen JA, Meschia JF, Levy S, Broderick DF, Graff-Radford N, Ross OA, Miller BB, Swerdlow RH, Dickson DW, Wszolek ZK. 2011. Mutations in the colony stimulating factor 1 receptor (CSF1R) gene cause hereditary diffuse leukoencephalopathy with spheroids. Nat Genet 44(2):200–205.

Richards A, van den Maagdenberg AM, Jen JC, Kavanagh D, Bertram P, Spitzer D, Liszewski MK, Barilla-Labarca ML, Terwindt GM, Kasai Y, McLellan M, Grand MG, Vanmolkot KR, de Vries B, Wan J, Kane MJ, Mamsa H, Schäfer R, Stam AH, Haan J, de Jong PT, Storimans CW, van Schooneveld MJ, Oosterhuis JA, Gschwendter A, Dichgans M, Kotschet KE, Hodgkinson S, Hardy TA, Delatycki MB, Hajj-Ali RA, Kothari PH, Nelson SF, Frants RR, Baloh RW, Ferrari MD, Atkinson JP. 2007. C-terminal truncations in human 3′–5′ DNA exonuclease TREX1 cause autosomal dominant retinal vasculopathy with cerebral leukodystrophy. Nat Genet 39(9):1068–1070.

Saito TL, Yoshimura J, Sasaki S, Ahsan B, Sasaki A, Kuroshu R, Morishita S. 2009. UTGB toolkit for personalized genome browsers. Bioinformatics 25(15):1856–1861.

Sakai N, Inui K, Fujii N, Fukushima H, Nishimoto J, Yanagihara I, Isegawa Y, Iwamatsu A, Okada S. 1994. Krabbe disease: Isolation and characterization of a full-length cDNA for human galactocerebrosidase. Biochem Biophys Res Commun 198(2):485–491.

Schwarz JM, Rödelsperger C, Schuelke M, Seelow D. 2010. MutationTaster evaluates disease-causing potential of sequence alterations. Nat Methods 7(8):575–576.

Sherrington R, Rogaev EI, Liang Y, Rogaeva EA, Levesque G, Ikeda M, Chi H, Lin C, Li G, Holman K, Tsuda T, Mar L, Foncin JF, Bruni AC, Montesi MP, Sorbi S, Rainero I, Pinessi L, Nee L, Chumakov I, Pollen D, Brookes A, Sanseau P, Polinsky RJ, Wasco W, Da Silva HA, Haines JL, Perkicak-Vance MA, Tanzi RE, Roses AD, Fraser PE, Rommens JM, St George-Hyslop PH. 1995. Cloning of a gene bearing missense mutations in early-onset familial Alzheimer's disease. Nature 375(6534):754–760.

Van Broeckhoven C, Haan J, Bakker E, Hardy JA, Van Hul W, Wehnert A, Vegter-Van der Vlis M, Roos RA. 1990. Amyloid beta protein precursor gene and hereditary cerebral hemorrhage with amyloidosis (Dutch). Science 248(4959):1120–1122.

van der Knaap MS, Naidu S, Kleinschmidt-Demasters BK, Kamphorst W, Weinstein HC. 2000. Autosomal dominant diffuse leukoencephalopathy with neuroaxonal spheroids. Neurology 54(2):463–468.

van der Knaap MS, Leegwater PA, Könst AA, Visser A, Naidu S, Oudejans CB, Schutgens RB, Pronk JC. 2002. Mutations in each of the five subunits of translation initiation factor eIF2B can cause leukoencephalopathy with vanishing white matter. Ann Neurol 51(2):264–270.

Van Gerpen JA, Wider C, Broderick DF, Dickson DW, Brown LA, Wszolek ZK. 2008. Insights into the dynamics of hereditary diffuse leukoencephalopathy with axonal spheroids. Neurology 71(12):925–929.

Vidal R, Frangione B, Rostagno A, Mead S, Révész T, Plant G, Ghiso J. 1999. A stop-codon mutation in the BRI gene associated with familial British dementia. Nature 399(6738):776–781.

Wider C, Van Gerpen JA, DeArmond S, Shuster EA, Dickson DW, Wszolek ZK. 2009. Leukoencephalopathy with spheroids (HDLS) and pigmentary leukodystrophy (POLD): A single entity? Neurology 72(22):1953–1959.

REPORT

The TRK-Fused Gene Is Mutated in Hereditary Motor and Sensory Neuropathy with Proximal Dominant Involvement

Hiroyuki Ishiura,[1] Wataru Sako,[3] Mari Yoshida,[4] Toshitaka Kawarai,[3] Osamu Tanabe,[3,5] Jun Goto,[1] Yuji Takahashi,[1] Hidetoshi Date,[1] Jun Mitsui,[1] Budrul Ahsan,[1] Yaeko Ichikawa,[1] Atsushi Iwata,[1] Hiide Yoshino,[6] Yuishin Izumi,[3] Koji Fujita,[3] Kouji Maeda,[3] Satoshi Goto,[3] Hidetaka Koizumi,[3] Ryoma Morigaki,[3] Masako Ikemura,[7] Naoko Yamauchi,[7] Shigeo Murayama,[8] Garth A. Nicholson,[9] Hidefumi Ito,[10] Gen Sobue,[11] Masanori Nakagawa,[12] Ryuji Kaji,[3,*] and Shoji Tsuji[1,2,13,*]

Hereditary motor and sensory neuropathy with proximal dominant involvement (HMSN-P) is an autosomal-dominant neurodegenerative disorder characterized by widespread fasciculations, proximal-predominant muscle weakness, and atrophy followed by distal sensory involvement. To date, large families affected by HMSN-P have been reported from two different regions in Japan. Linkage and haplotype analyses of two previously reported families and two new families with the use of high-density SNP arrays further defined the minimum candidate region of 3.3 Mb in chromosomal region 3q12. Exome sequencing showed an identical c.854C>T (p.Pro285-Leu) mutation in the TRK-fused gene (*TFG*) in the four families. Detailed haplotype analysis suggested two independent origins of the mutation. Pathological studies of an autopsied patient revealed TFG- and ubiquitin-immunopositive cytoplasmic inclusions in the spinal and cortical motor neurons. Fragmentation of the Golgi apparatus, a frequent finding in amyotrophic lateral sclerosis, was also observed in the motor neurons with inclusion bodies. Moreover, TAR DNA-binding protein 43 kDa (TDP-43)-positive cytoplasmic inclusions were also demonstrated. In cultured cells expressing mutant TFG, cytoplasmic aggregation of TDP-43 was demonstrated. These findings indicate that formation of TFG-containing cytoplasmic inclusions and concomitant mislocalization of TDP-43 underlie motor neuron degeneration in HMSN-P. Pathological overlap of proteinopathies involving TFG and TDP-43 highlights a new pathway leading to motor neuron degeneration.

Hereditary motor and sensory neuropathy with proximal dominant involvement (HMSN-P [MIM 604484]) is an autosomal-dominant disease characterized by predominantly proximal muscle weakness and atrophy followed by distal sensory disturbances.[1] HMSN-P was first described in patients from the Okinawa Islands of Japan, where more than 100 people are estimated to be affected.[2] Two Brazilian HMSN-P-affected families of Okinawan ancestry have also been reported.[3,4]

The disease onset is usually in the 40s and is followed by a slowly progressive course. Painful muscle cramps and abundant fasciculations are observed, particularly in the early stage of the disease. In contrast to the clinical presentations of other hereditary motor and sensory neuropathies (HMSNs) presenting with predominantly distal motor weakness reflecting axonal-length dependence, the clinical presentation of HMSN-P is unique in that it involves proximal predominant weakness with widespread fasciculations resembling those of amyotrophic lateral sclerosis (ALS).[5] Distal sensory loss is accompanied later in the disease course, but the degree of the sensory involvement varies among patients. Neuropathological findings revealed severe neuronal loss and gliosis in the spinal anterior horns and mild neuronal loss and gliosis in the hypoglossal and facial nuclei of the brainstem, which indicates that the primary pathological feature of HMSN-P is a motor neuronopathy involving motor neurons, but not a motor neuropathy involving axons.[1,5] The posterior column, corticospinal tract, and spinocerebellar tract showed loss of myelinated fibers and gliosis. Neuronal loss and gliosis were found in Clarke's nucleus. Dorsal root ganglia showed mild to marked neuronal loss.[1,5] These observations suggest that HMSN-P shares neuropathological findings in part with those observed in familial ALS.[6]

Previous studies on Okinawan kindreds mapped the disease locus to chromosome 3q.[1] Subsequently, we identified two large families (families 1 and 2 in Figure 1A) affected by quite a similar phenotype in the Kansai area of Japan, located in the middle of the main island of Japan and far distant from the Okinawa Islands. We mapped the

[1]Department of Neurology, The University of Tokyo Graduate School of Medicine, 7-3-1 Hongo, Bunkyo-ku, Tokyo 113-8655, Japan; [2]Medical Genome Center, The University of Tokyo Hospital, 7-3-1 Hongo, Bunkyo-ku, Tokyo 113-8655, Japan; [3]Department of Clinical Neuroscience, The Tokushima University Graduate School of Medicine, 3-18-15 Kuramoto-cho, Tokushima 770-8503, Japan; [4]Department of Neuropathology, Institute for Medical Science of Aging, Aichi Medical University, 21 Karimata, Iwasaku, Nagakute-shi, Aichi 480-1195, Japan; [5]Department of Cell and Developmental Biology, University of Michigan Medical School, 109 Zina Pitcher Place, Ann Arbor, MI 48109-2200, USA; [6]Yoshino Neurology Clinic, 3-3-16 Konodai, Ichikawa, Chiba 272-0827, Japan; [7]Department of Pathology, Graduate School of Medicine, The University of Tokyo, 7-3-1 Hongo, Bunkyo-ku, Tokyo 113-8655, Japan; [8]Department of Neuropathology and the Brain Bank for Aging Research, Tokyo Metropolitan Institute of Gerontology, 35-2 Sakae-cho, Itabashi-ku, Tokyo 173-0015, Japan; [9]Molecular Medicine Laboratory and ANZAC Research Institute, University of Sydney, Sydney NSW 2139, Australia; [10]Department of Neurology, Kyoto University Graduate School of Medicine, 54 Kawahara-cho, Shogoin, Sakyo-ku, Kyoto 606-8507, Japan; [11]Department of Neurology, Nagoya University Graduate School of Medicine, 65 Tsurumai-cho, Showa-ku, Nagoya-shi, Aichi 466-0065, Japan; [12]Department of Neurology and Gerontology, Kyoto Prefectural University Graduate School of Medicine, 465, Kajii-cho, Kamigyo-ku, Kyoto 602-0841, Japan; [13]Division of Applied Genetics, National Institute of Genetics, Yata 1111, Mishima, Shizuoka 11-8540, Japan
*Correspondence: tsuji@m.u-tokyo.ac.jp (S.T.), rkaji@clin.med.tokushima-u.ac.jp (R.K.)
http://dx.doi.org/10.1016/j.ajhg.2012.07.014.

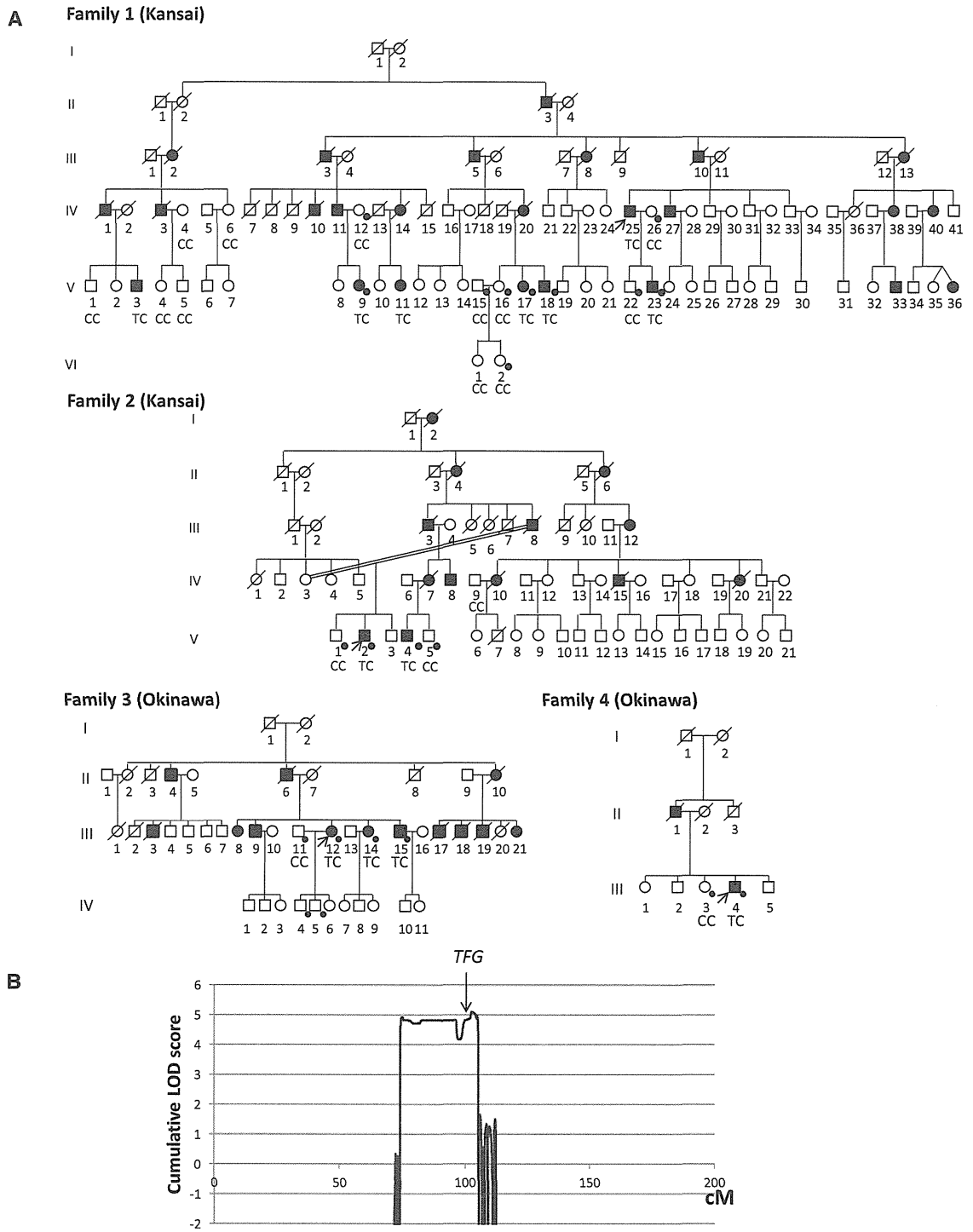

Figure 1. Pedigree Charts and Linkage Analysis
(A) Pedigree charts of families 1 and 2 (Kansai kindreds) and families 3 and 4 (Okinawan kindreds) are shown. Squares and circles indicate males and females, respectively. Affected persons are designated with filled symbols. A diagonal line through a symbol represents a deceased person. A person with an arrow is an index patient. Genotypes of *TFG* c.854 are shown in individuals in whom genomic DNA was analyzed. Individuals genotyped with SNP arrays for linkage analysis and haplotype reconstruction are indicated by dots.
(B) Cumulative parametric multipoint LOD scores on chromosome 3 of all the families are shown.

disease locus to chromosome 3q,[7] overlapping with the previously defined locus, which strongly indicates that these diseases are indeed identical.

In addition to the large Kansai HMSN-P-affected families, we found two new Okinawan HMSN-P-affected families (families 3 and 4 in Figure 1A) in our study. In total, 9 affected and 15 unaffected individuals from the Kansai area and four affected and four unaffected individuals from the Okinawa Islands were enrolled in the study. Written informed consent was obtained from

Table 1. Clinical Characteristics of Patients with HMSN-P from Families 1 and 2 from Kansai and Families 3 and 4 from Okinawa

		Family 3			Family 4
	Families 1 and 2	III-12	III-14	III-15	III-4
Age at examination (years)	40s–50s	54	52	50	54
Age at onset (years)	37.5 ± 8	44	40	early 20s	41
Initial symptoms	shoulder dislocation and difficulty walking	proximal leg weakness	painful cramps	painful cramps and fasciculation	painful cramps and calf atrophy
Motor					
Proximal muscle weakness and atrophy	+	+	mild	+	+
Painful cramps	+	+	+	+	+
Fasciculations	+	+	+	+	+
Motor ability	bedridden after 10–20 years from disease onset	unable to walk; wheelchair	only mild difficulty climbing stairs	walk with effort	unable to walk; wheelchair
Bulbar symptoms	− ~ +	−	−	−	−
Sensory					
Dysesthesia	+	+	mild	+	+
Decreased tactile sensation	+	+	−	mild	+
Decreased vibratory sensation	+	mild	mild	mild	+
Reflexes					
Tendon reflexes	diminished	diminished	diminished	diminished	diminished
Pathological reflexes	−	−	−	−	−
Laboratory Tests and Electrophysiological Findings					
Serum creatine kinase level	270 ± 101 IU/l	761 IU/l	not measured	625 IU/l	399 IU/l
Hyperglycemia	4/13 patients	−	−	−	+
Hyperlipidemia	3/13 patients	+	−	+	+
Nerve conduction study	motor and sensory axonal degeneration	motor and sensory axonal degeneration	not examined	not examined	motor and sensory axonal degeneration
Needle electromyography	neurogenic changes with fibrillation potentials and positive sharp waves	neurogenic changes with fibrillation potentials and positive sharp waves	not examined	not examined	not examined

The clinical characteristics of the patients from families 1 and 2 were summarized in accordance with the previous studies.[5,6]

all participants. This study was approved by the institutional review boards at the University of Tokyo and the Tokushima University Hospital. Genomic DNA was extracted from peripheral-blood leukocytes or an autopsied brain according to standard procedures.

The clinical presentations of the patients from the four families are summarized in Table 1 and Table S1, available online. Characteristic painful cramps and fasciculations were noted at the initial stage of the disease in all the patients from the four families. Whereas some of the patients showed painful cramps in their 20s, the ages of onset of motor weakness (41.6 ± 2.9 years old) were quite uniform. These patients presented slowly progressive, predominantly proximal weakness and atrophy with diminished tendon reflexes in the lower extremities. Sensory impairment was generally mild. Indeed, one patient (III-4 in family 4) has been diagnosed with very slowly progressive ALS. Although frontotemporal dementia (FTD) is an occasionally observed clinical presentation in patients with ALS, dementia was not observed in these patients. Laboratory tests showed mildly elevated serum creatine kinase levels. Electrophysiological studies showed similar results in all the patients investigated and revealed a decreased number of motor units with abundant positive sharp waves, fibrillation, and fasciculation potentials. Sensory-nerve action potentials of the sural nerve were lost in the later stage of the disease. All these clinical findings were similar to those described in previous reports.[1,3,4]

To further narrow the candidate region, we conducted detailed genotyping by employing the Genome-Wide Human SNP array 6.0 (Affymetrix). Multipoint parametric linkage analysis and haplotype reconstruction were performed with the pipeline software SNP-HiTLink[8] and Allegro v.2[9] (Figure 1A). In addition to the SNP genotyping, we also used newly discovered polymorphic dinucleotide repeats for haplotype comparison (microsatellite marker 1 [MS1], chr3: 101,901,207–101,901,249; and MS2, chr3: 102,157,749–102,157,795 in hg18) around *TFG* (see Table S2 for primer sequences). The genome-wide linkage study revealed only one chromosome 3 region showing a cumulative LOD score exceeding 3.0 (Figure 1B), confirming the result of our previous study.[7] An obligate recombination event was observed between rs4894942 and rs1104964, thus further refining the telomeric boundary of the candidate region in Kansai families (Figure 2A). The Okinawan families (families 3 and 4) shared an extended disease haplotype spanning 3.3 Mb, consistent with a founder effect reported in the Okinawan HMSN-P-affected families,[1] thus defining the 3.3 Mb region as the minimum candidate region.

We then performed exon capture (Sequence Capture Human Exome 2.1 M Array [NimbleGen]) of the index patient from family 3 and subsequent passively parallel sequencing by using two lanes of GAIIx (100 bp single end [Illumina]) and a one-fifth slide of SOLiD 4 (50 bp single end [Life Technologies]). GAIIx and SOLiD4 yielded 2.60 and 2.76 Gb of uniquely mapped reads,[10] respectively. The average coverages were 29.0× and 26.8× in GAIIx and SOLiD4, respectively (Table S3 and Figure S1). In summary, 175,236 single nucleotide variants (SNVs) and 25,987 small insertions/deletions were called.[11] The numbers of exonic and splice-site variants were 14,189 and 127, respectively. In the minimum candidate region of 3.3 Mb, only 11 exonic SNVs were found, and only one was novel (i.e., not found in dbSNP) and nonsynonymous. Direct nucleotide-sequence analysis confirmed the presence of heterozygous SNV c.854C>T (p.Pro285Leu) in TRK-fused gene (*TFG* [NM_006070.5]) in all the patients from families 3 and 4 (Figure 3A and Figure S2[12]). Intriguingly, direct nucleotide-sequence analysis of all *TFG* exons (see Table S4 for primer sequences) of one patient from each of families 1 and 2 from the Kansai area revealed an identical c.854C>T (p.Pro285Leu) *TFG* mutation cosegregating with the disease (Figure 1A and Figure 3A). The base substitution was not observed in 482 Japanese controls (964 chromosomes), dbSNP, the 1000 Genomes Project Database, or the Exome Sequencing Project Database. Pro285 is located in the P/Q-rich domain in the C-terminal region of TFG (Figure 3B) and is evolutionally conserved (Figure 3C). PolyPhen predicts it to be "probably damaging." Because some of the exonic sequences were not sufficiently covered by exome sequencing (i.e., their read depths were no more than 10×) (Figure S1), direct nucleotide-sequence analysis was further conducted for these exonic sequences (Table S5). However, it did not reveal any other novel nonsynonymous variants, confirming that c.854C>T (p.Pro285Leu) is the only mutation exclusively present in the candidate region of 3.3 Mb. All together, we concluded that it was the disease-causing mutation.

Because we found an identical mutation in both Kansai (families 1 and 2) and Okinawan (families 3 and 4) families, we then compared the haplotypes with the c.854C>T (p.Pro285Leu) mutation in the Kansai and Okinawan families in detail. To obtain high-resolution haplotypes, we included custom-made markers, including MS1 and MS2, and new SNVs identified by our exome analysis, in addition to the high-density SNPs used in the linkage analysis. The two Kansai families shared as long as 24.0 Mb of haplotype, and the two Okinawan families shared 3.3 Mb, strongly supporting a common ancestry in each region. When the haplotypes of the Kansai and Okinawan families were compared, it turned out that these families do not share the same haplotype because the markers nearest to *TFG* are discordant at markers 48.5 kb centromeric and 677 bp telomeric to the mutation within a haploblock (Figure 2B). Although the possibility of rare recombination events just distal to the mutation cannot be completely excluded, as suggested by the population-based recombination map (Figure 2B), these findings strongly support the interpretation that the mutations have independent origins and provide further evidence that *TFG* contains the causative mutation for this disease.

Mutational analyses of *TFG* were further conducted in patients with other diseases affecting lower motor neurons (including familial ALS [n = 18], axonal HMSN [n = 26], and hereditary motor neuropathy [n = 3]) and revealed no mutations in *TFG*, indicating that c.854C>T (p.Pro285Leu) in *TFG* is highly specific to HMSN-P.

In this study, we identified in all four families a single variant that appears to have developed on two different haplotypes. The mutation disrupts the PXXP motif, also known as the Src homology 3 (SH3) domain, which might affect protein-protein interactions. In addition, substitution of leucine for proline is expected to markedly alter the protein's secondary structure, which might substantially compromise the physiological functions of TFG.

By employing the primers shown in Table S6, we obtained full-length cDNAs by PCR amplification of the cDNAs prepared from a cDNA library of the human fetal brain (Clontech). During this process, four species of cDNA were identified (Figure S3A). To determine the relative abundance of these cDNA species, we used the primers shown in Table S7 to conduct fragment analysis of the RT-PCR products obtained from RNAs extracted from various tissues; these primers were designed to discriminate four cDNA species on the basis of the size of the PCR products. The analysis revealed that TFG is ubiquitously expressed, including in the spinal cord and dorsal root ganglia, which are the affected sites of HMSN-P (Figure S3B).

Neuropathological studies were performed in a *TFG*-mutation-positive patient (IV-25 in family 1) who died of

A

Chromosomal Position (hg18)	Marker	Kansai Type		Okinawa Type	
		Family 1	Family 2	Family 3	Family 4
99,780,627	rs9283596	A	A	A	G
100,433,654	rs16840796	A	A	T	A
100,953,998	rs792841	G	(G/T)	T	T
100,957,958	rs792833	G	(A/G)	A	A
100,966,463	rs704574	T	(C/T)	C	C
101,066,174	rs1718235	C	(C/T)	T	T
101,687,648	rs4928088	T	T	C	(C/T)
101,901,207 ~ 101,901,249	MS1	313	313	309	(309/315)
101,949,716	*TFG* c.854C>T	T	T	T	T
101,950,393	ss532644308	C	C	T	T
101,968,141	rs544500	T	T	C	C
101,977,868	rs16842822	C	C	G	G
101,982,011	rs7613610	T	T	G	G
101,994,136	rs989795	T	T	A	A
102,008,560	rs1503845	G	G	A	A
102,058,443	rs6780804	C	(C/T)	T	T
102,157,749 ~ 102,157,795	MS2	347	347	339	339
103,742,115	rs9854367	A	A	A	A
103,742,427	rs1284730	A	A	G	A
104,468,183	rs10937358	C	C	C	T
104,496,273	rs13061385	C	C	C	A
105,356,604	rs4894942	T	T	T	T
105,373,669	rs1104964	G	A	A	(A/G)

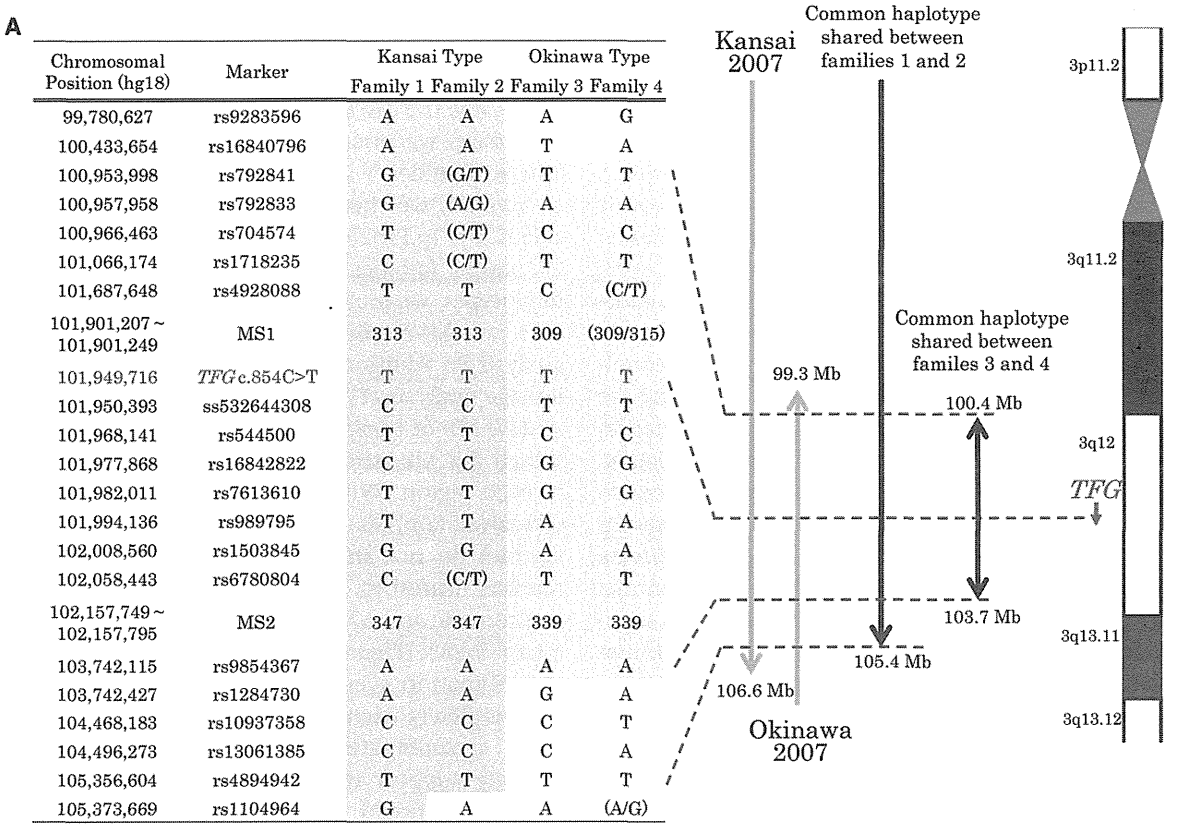

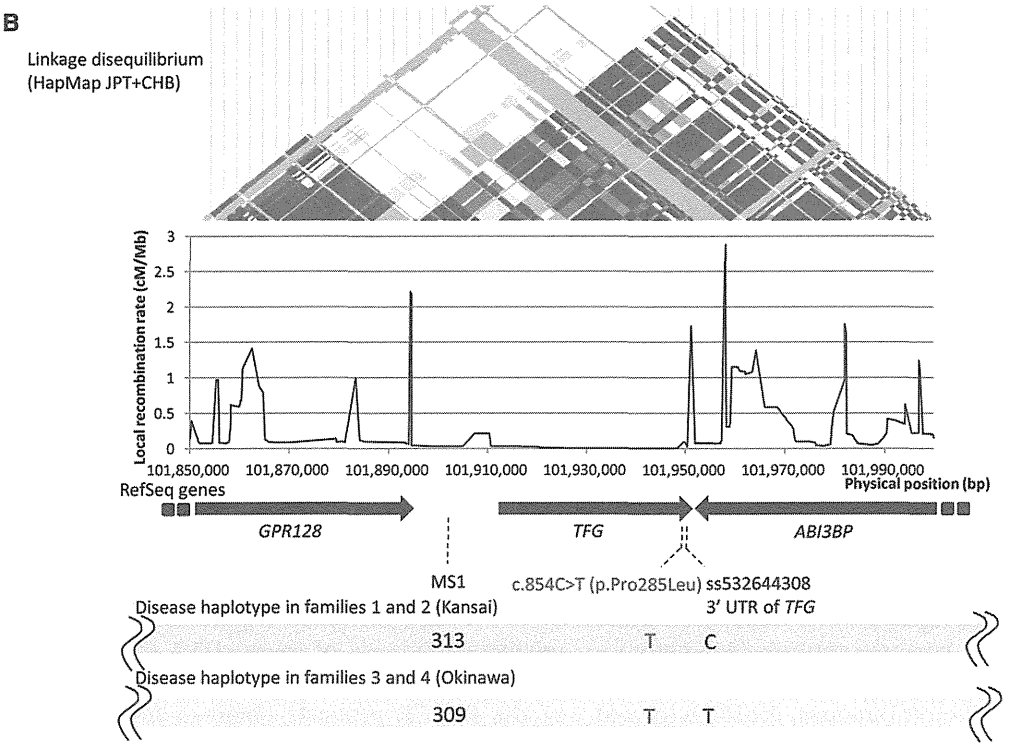

Figure 2. Haplotype Analysis and Minimum Candidate Region of HMSN-P
(A) Haplotypes were reconstructed for all the families with the use of SNP array data and microsatellite markers. Previously reported candidate regions are shown as "Kansai 2007" and "Okinawa 2007."[1,6] Because families 1 and 2 are distantly related, an extended shared common haplotype was observed on chromosome 3, as indicated by a previous study.[6] A reassessment of linkage analysis with high-density SNP markers revealed a recombination between rs4894942 and rs1104964 in family 2, thus refining the telomeric boundary of the candidate region in Kansai families (designated as "Common haplotype shared between families 1 and 2). Furthermore, a shared common haplotype (3.3 Mb with boundaries at rs16840796 and rs1284730) between families 3 and 4 was found, defining the minimum candidate region.

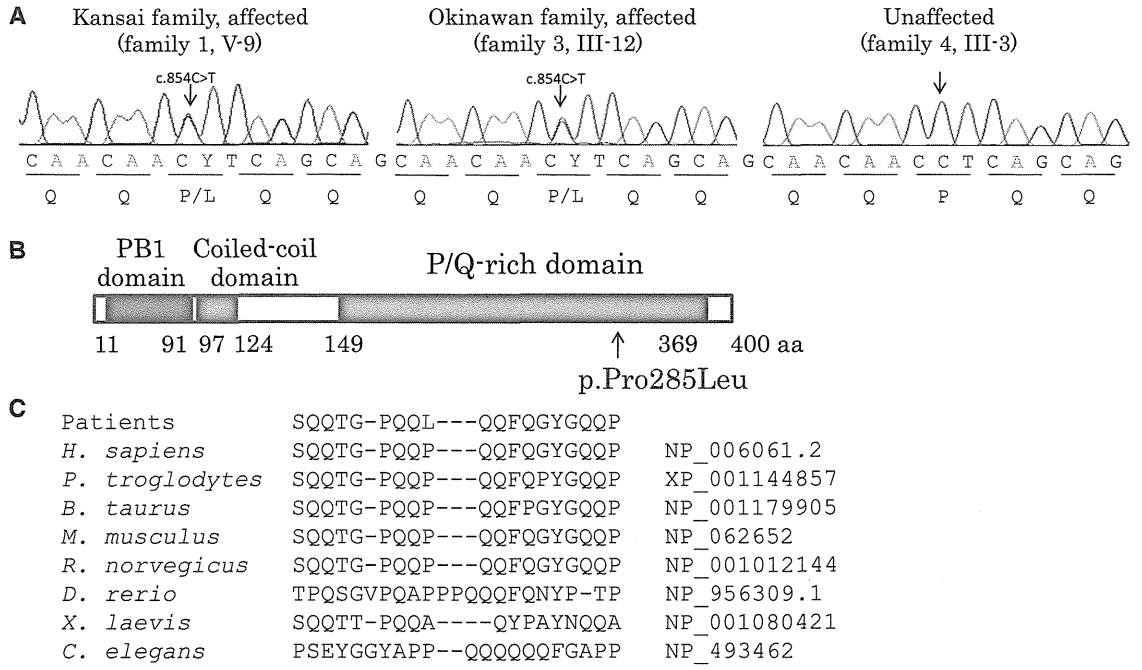

Figure 3. Identification of Causative Mutation

(A) Exome sequencing revealed that only one novel nonsynonymous variant is located within the minimum candidate region. Direct nucleotide-sequence analysis confirmed the mutation, c.854C>T (p.Pro285Leu), in *TFG* in both Kansai and Okinawan families. The mutation cosegregated with the disease (Figure 1A).

(B) Schematic representation of TFG isoform 1. The alteration (p.Pro285Leu) detected in this study is shown below.

(C) Cross-species homology search of the partial TFG amino acid sequence containing the p.Pro285Leu alteration revealed that Pro285 is evolutionally conserved among species.

pneumonia at 67 years of age.[5] Immunohistochemical observations employing a TFG antibody (Table S8) revealed fine granular immunostaining of TFG in the cytoplasm of motor neurons in the spinal cord of neurologically normal controls (n = 3; age at death = 58.7 ± 19.6 years old) (Figure 4A). In the HMSN-P patient, in contrast, TFG-immunopositive inclusion bodies were detected in the motor neurons of the facial, hypoglossal, and abducens nuclei and the spinal cord, as well as in the sensory neurons of the dorsal root ganglia, but were not detected in glial cells (Figures 4B–4D). A small number of cortical neurons in the precentral gyrus also showed TFG-immunopositive inclusion bodies (Figure 4E). Serial sections stained with antibodies against ubiquitin or TFG (Figure 4F) and double immunofluorescence staining (Figure 4G) demonstrated that TFG-immunopositive inclusions colocalized with ubiquitin deposition. Inclusion bodies were immunopositive for optineurin in motor neurons of the brainstem nuclei and the anterior horn of the spinal cord,[5] as well as in sensory neurons of the dorsal root ganglia (data not shown). These data strongly indicate that HMSN-P is a proteinopathy involving TFG.

Because HMSN-P and ALS share some clinical characteristics, we then examined whether neuropathological findings of HMSN-P shared cardinal features with those of sporadic ALS.[13–16] Immunohistochemistry with a TDP-43 antibody revealed skein-like inclusions in the remaining motor neurons of the abducens nucleus and the anterior horn of the lumbar cord (Figures 4H–4I). Phosphorylated TDP-43-positive inclusions were also identified in neurons of the anterior horn of the cervical cord and Clarke's nucleus (Figures 4J–4K). In contrast, TFG immunostaining of spinal-cord specimens from four patients with sporadic ALS (their age at death was 72.3 ± 7.4 years old) revealed no pathological staining in the motor neurons (data not shown). Double immunofluorescence staining revealed that many of the TFG-immunopositive round inclusions in the HSMN-P patient were negative for TDP-43 (Figure 4L), whereas a small number of inclusions were positive for both TFG and TDP-43 (Figure 4M). In addition, to investigate morphological Golgi-apparatus changes, which have recently been found in motor neurons of autopsied tissues of ALS patients,[17] we conducted immunohistochemical analysis by using

(B) Disease haplotypes in the Kansai and Okinawan kindreds are indicated below. Local recombination rates, RefSeq genes, and the linkage disequilibrium map from HapMap JPT (Japanese in Tokyo, Japan) and CHB (Han Chinese in Beijing, China) samples are shown above the disease haplotypes. When disease haplotypes of the Kansai and Okinawan kindreds are compared, the markers nearest to *TFG* are discordant at markers 48.5 kb centromeric and 677 bp telomeric to the mutation within a haploblock, strongly supporting the interpretation that the mutations have independent origins.

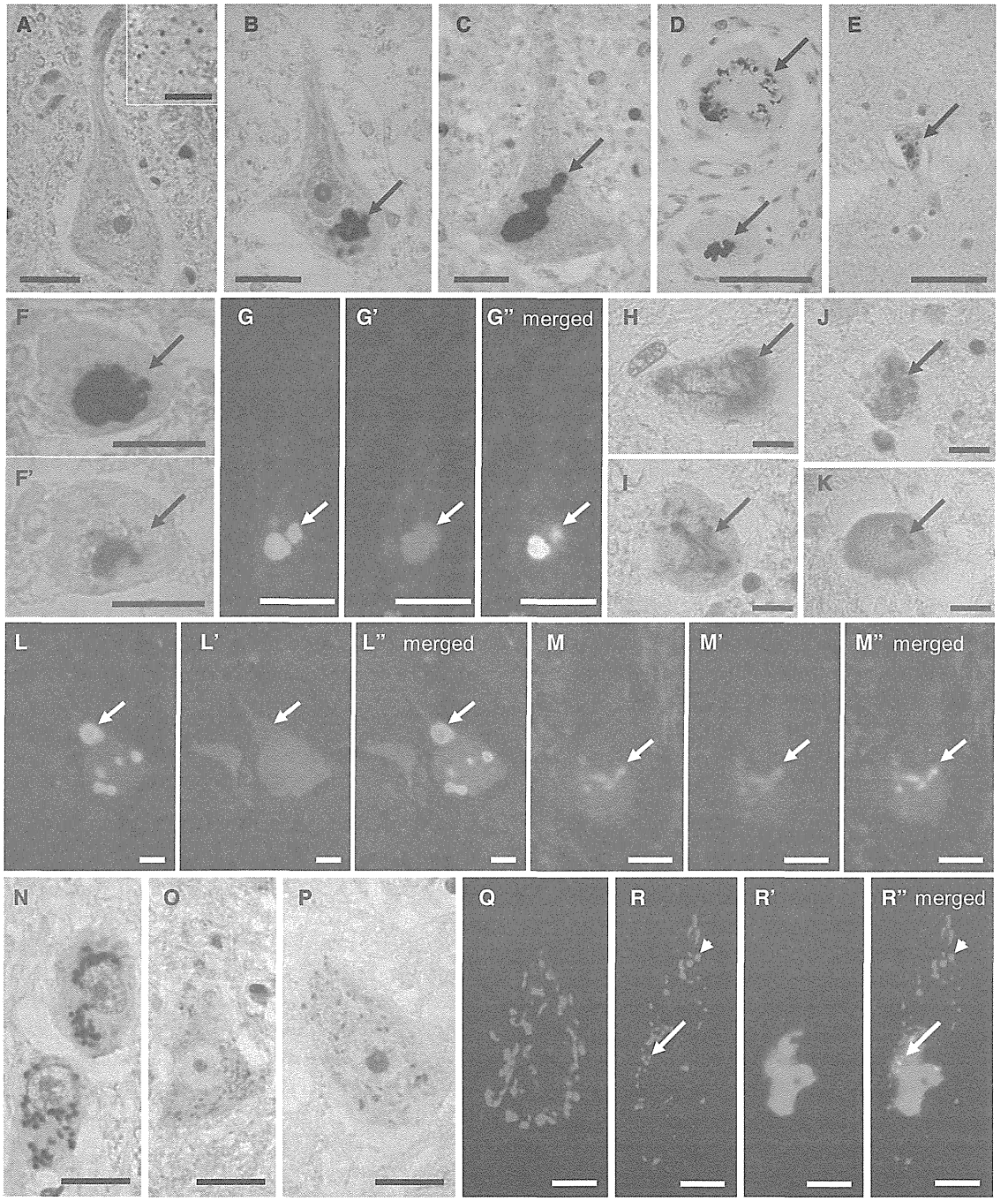

Figure 4. TFG-Related Neuropathological Findings

(A) TFG immunostaining (with hematoxylin counterstaining) of a motor neuron in the spinal cord of a neurologically normal control. A high-power magnified photomicrograph (inset) shows fine granular staining of TFG in the cytoplasm. The scale bars represent 20 μm (main panel) and 10 μm (inset).

(B–E) TFG-immunopositive inclusions of the neurons (with hematoxylin counterstaining) in the hypoglossal nucleus (B), anterior horn of the spinal cord (C), dorsal root ganglion (D, arrows), and motor cortex (E, arrow) of the patient with the *TFG* mutation. The scale bars represent 20 μm (B–D) and 50 μm (E).

(F and F′) Serial section analysis of the facial nucleus motor neuron showing an inclusion body colabeled for TFG (F) and ubiquitin (F′). The scale bars represent 20 μm.

(G–G″) Double immunofluorescence microscopy confirming colocalization of TFG (green) and ubiquitin (red) in an inclusion body of a motor neuron in the hypoglossal nucleus. The scale bars represent 20 μm.

(H and I) TDP-43-positive skein-like inclusions in the motor neurons of the abducens nucleus (H) and anterior horn of the lumbar cord (I). The scale bars represent 20 μm.

(J and K) Phosporylated TDP-43-positive inclusion bodies in the cervical anterior horn (J) and Clarke's nucleus (K). The scale bars represent 20 μm.

(L–L″) Round inclusions (arrows) positive for TFG (green) but negative for TDP-43 (red). The scale bars represent 20 μm.

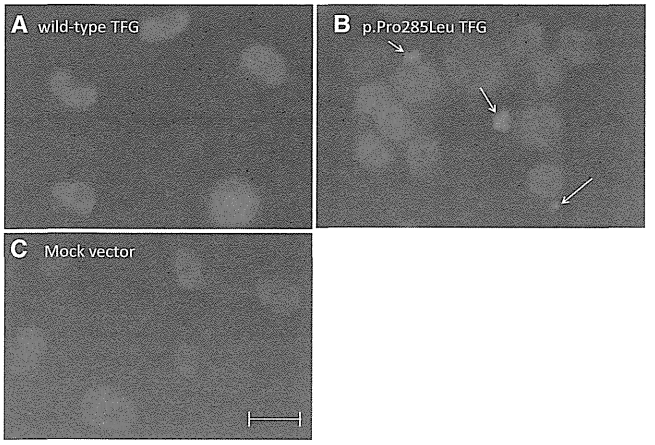

Figure 5. Formation of Cytoplasmic TDP-43 Aggregation Bodies in Cells Stably Expressing Mutant p.Pro285Leu TFG
The coding sequence of *TFG* cDNA was subcloned into pBluescript (Stratagene). After site-directed mutagenesis with a primer pair shown in Table S9, the mutant cDNAs were cloned into the BamHI and XhoI sites of pcDNA3 (Life Technologies). Stable cell lines were established by Lipofectamine (Life Technologies) transfection according to the manufacturer's instructions. Established cell lines were cultured under the ordinary cell-culture conditions (37°C and 5% CO_2) for 5–6 days and were subjected to immunocytochemical analyses. Neuro-2a cells stably expressing wild-type TFG (A), mutant TFG (p.Pro285Leu) (B), and a mock vector (C) are shown. TDP-43-immunopositive cytoplasmic inclusions are absent in the cells stably expressing wild-type TFG or the mock vector (A and C); however, TDP-43-immunopositive cytoplasmic inclusions were exclusively demonstrated in cells stably expressing mutant TFG (p.Pro285Leu), as indicated by arrows (B). Similar results were obtained with HEK 293 cells (not shown). Scale bars represent 10 μm.

a TGN46 antibody. It revealed that the Golgi apparatus was fragmented in approximately 70% of the remaining motor neurons in the lumbar anterior horn. The fragmentation of the Golgi apparatus was prominent near TFG-positive inclusion bodies (Figures 4N–4R). In summary, we found abnormal TDP-43-immunopositive inclusions in the cytoplasm of motor neurons, as well as fragmentation of the Golgi apparatus in HMSN-P, confirming the overlapping neuropathological features between HMSN-P and sporadic ALS.

To further investigate the effect of mutant TFG in cultured cells, stable cell lines expressing wild-type and mutant TFG (p.Pro285Leu) were established from neuro-2a and human embryonic kidney (HEK) 293 cells as previously described.[18] Established cell lines were cultured under the ordinary cell-culture conditions (37°C and 5% CO_2) for 5–6 days and were subjected to immunocytochemical analyses. The neuro-2a cells stably expressing wild-type or mutant TFG demonstrated no distinct difference in the distribution of endogenous TFG, FUS, or OPTN (data not shown). In contrast, cytoplasmic inclusions containing endogenous TDP-43 were exclusively observed in the neuro-2a cells stably expressing untagged mutant TFG, but not in those expressing wild-type TFG (Figure 5). Similar data were obtained from HEK 293 cells (data not shown). Thus, the expression of mutant TFG leads to mislocalization and inclusion-body formation of TDP-43 in cultured cells.

TFG was originally identified as a part of fusion oncoproteins (NTRK1-T3 in papillary thyroid carcinoma,[19] TFG-ALK in anaplastic large cell lymphoma,[20] and TFG/NOR1 in extraskeletal myxoid chondrosarcoma[21]), where the N-terminal portions of TFG are fused to the C terminus of tyrosine kinases or a superfamily of steroid-thyroid hormone-retinoid receptors acting as a transcriptional activator leading to the formation of oncogenic products. Very recently, TFG-1, a homolog of TFG in *Caenorhabditis elegans*, and TFG have been discovered to localize in endoplasmic-reticulum exit sites. TFG-1 acts in a hexameric form that binds the scaffolding protein Sec16 complex assembly and plays an important role in protein secretion with COPII-coated vesicles.[22] It is noteworthy that mutations in genes involved in vesicle trafficking[23,24] (such genes include *VAPB*, *CHMP2B*, *alsin*, *FIG4*, *VPS33B*, *PIP5K1C*, and *ERBB3*) cause motor neuron diseases, emphasizing the role of vesicle trafficking in motor neuron diseases. Thus, altered vesicle trafficking due to the *TFG* mutation might be involved in the motor neuron degeneration in HMSN-P. The presence of TFG-immunopositive inclusions in motor neurons raises the possibility that mutant TFG results in the misfolding and formation of cytoplasmic aggregate bodies, as well as altered vesicle trafficking.

An intriguing neuropathological finding is TDP-43-positive cytoplasmic inclusions in the motor neurons; these inclusions have recently been established as the fundamental neuropathological findings in ALS.[13,14] Of note, expression of mutant, but not wild-type, TFG in cultured cells led to the formation of TDP-43-containing cytoplasmic aggregation. These observations are similar

(M–M″) An inclusion immunopositive for both TFG (green) and TDP-43 (red) is observed in a small number of neurons. The scale bars represent 20 μm.
(N) Normal Golgi apparatus in the neurons of the intact thoracic intermediolateral nucleus. The scale bar represents 20 μm.
(O and P) Fragmentation of the Golgi apparatus with small, round, and disconnected profiles in the affected motor neurons of the lumbar anterior horn. The scale bars represent 20 μm.
(Q–R″) Immunohistochemical observations of the Golgi apparatus and TFG-immunopositive inclusions employing antibodies against TGN46 (red) and TFG (green), respectively. The scale bars represent 10 μm.
(Q) Normal size and distribution (red) in a motor neuron without inclusions.
(R–R″) The Golgi apparatus was fragmented into various sizes and reduced in number in the lumbar anterior horn motor neuron with TFG-positive inclusions (green). The fragmentation predominates near the inclusion (arrow), whereas the Golgi apparatuses distant from the inclusion showed nearly normal patterns (arrow head).

to what has been described for ALS, where TDP-43 is mislocalized from the normally localized nucleus to the cytoplasm with concomitant cytoplasmic inclusions. Cytoplasmic TDP-43 accumulation and inclusion formation have also been observed in motor neurons in familial ALS with mutations in *VAPB* (MIM 608627) or *CHMP2B* (MIM 600795).[25,26] Furthermore, TDP-43 pathology has been demonstrated in transgenic mice expressing mutant VAPB.[27] Although the mechanisms of mislocalization of TDP-43 remain to be elucidated, these observations suggest connections between alteration of vesicle trafficking and mislocalization of TDP-43. Thus, common pathophysiologic mechanisms might underlie motor neuron degenerations involving vesicle trafficking including TFG, as well as VAPB and CHMP2B. Because TDP-43 is an RNA-binding protein, RNA dysregulation has been suggested to play important roles in the TDP43-mediated neurodegeneration.[28] Furthermore, recent discovery of hexanucleotide repeat expansions in *C9ORF72* in familial and sporadic ALS/FTD (MIM 105550)[29,30] emphasizes the RNA-mediated toxicities as the causal mechanisms of neurodegeneration. Observations of TDP-43-positive cytoplasmic inclusions in the motor neurons of the patient with HMSN-P raise the possibility that RNA-mediated mechanisms might also be involved in motor neuron degeneration in HMSN-P.

In summary, we have found that *TFG* mutations cause HMSN-P. The presence of TFG/ubiquitin- and/or TDP-43-immunopositive cytoplasmic inclusions in motor neurons and cytosolic aggregation composed of TDP-43 in cultured cells expressing mutant TFG indicate a novel pathway of motor neuron death.

Supplemental Data

Supplemental Data include three figures and nine tables and can be found with this article online at http://www.cell.com/AJHG/.

Acknowledgments

The authors thank the families for participating in the study. We also thank the doctors who obtained clinical information of the patients. This work was supported in part by Grants-in-Aid for Scientific Research on Innovative Areas (22129002); the Global Centers of Excellence Program; the Integrated Database Project; Scientific Research (A) (B21406026) and Challenging Exploratory Research (23659458) from the Ministry of Education, Culture, Sports, Science, and Technology of Japan; a Grant-in-Aid for Research on Intractable Diseases and Comprehensive Research on Disability Health and Welfare from the Ministry of Health, Labour, and Welfare, Japan; Grants-in-Aid from the Research Committee of CNS Degenerative Diseases; the Ministry of Health, Labour, and Welfare of Japan; the Charcot-Marie-Tooth Association; and the National Medical Research Council of Australia. H.I. was supported by a Research Fellowship from the Japan Society for the Promotion of Science for Young Scientists. We also thank S. Ogawa (Cancer Genomics Project, The University of Tokyo) for his kind help in the analyses employing GAIIx and SOLiD4.

Received: April 16, 2012
Revised: May 27, 2012
Accepted: July 2, 2012
Published online: August 9, 2012

Web Resources

The URLs for data presented herein are as follows.

1000 Genomes Project Database, http://www.1000genomes.org/
dbSNP, http://www.ncbi.nlm.nih.gov/projects/SNP/
HapMap, http://hapmap.ncbi.nlm.nih.gov/
NHLBI GO Exome Sequencing Project, https://esp.gs.washington.edu/drupal/
Online Mendelian Inheritance in Man (OMIM), http://www.omim.org
PolyPhen, http://genetics.bwh.harvard.edu/pph/
RefSeq, http://www.ncbi.nlm.nih.gov/projects/RefSeq/
UCSC Human Genome Browser, http://genome.ucsc.edu/

References

1. Takashima, H., Nakagawa, M., Nakahara, K., Suehara, M., Matsuzaki, T., Higuchi, I., Higa, H., Arimura, K., Iwamasa, T., Izumo, S., and Osame, M. (1997). A new type of hereditary motor and sensory neuropathy linked to chromosome 3. Ann. Neurol. *41*, 771–780.
2. Nakagawa, M. (2009). [Wide spectrum of hereditary motor sensory neuropathy (HMSN)]. Rinsho Shinkeigaku *49*, 950–952.
3. Maeda, K., Sugiura, M., Kato, H., Sanada, M., Kawai, H., and Yasuda, H. (2007). Hereditary motor and sensory neuropathy (proximal dominant form, HMSN-P) among Brazilians of Japanese ancestry. Clin. Neurol. Neurosurg. *109*, 830–832.
4. Patroclo, C.B., Lino, A.M., Marchiori, P.E., Brotto, M.W., and Hirata, M.T. (2009). Autosomal dominant HMSN with proximal involvement: new Brazilian cases. Arq. Neuropsiquiatr. *67* (3B), 892–896.
5. Fujita, K., Yoshida, M., Sako, W., Maeda, K., Hashizume, Y., Goto, S., Sobue, G., Izumi, Y., and Kaji, R. (2011). Brainstem and spinal cord motor neuron involvement with optineurin inclusions in proximal-dominant hereditary motor and sensory neuropathy. J. Neurol. Neurosurg. Psychiatry *82*, 1402–1403.
6. Takahashi, H., Makifuchi, T., Nakano, R., Sato, S., Inuzuka, T., Sakimura, K., Mishina, M., Honma, Y., Tsuji, S., and Ikuta, F. (1994). Familial amyotrophic lateral sclerosis with a mutation in the Cu/Zn superoxide dismutase gene. Acta Neuropathol. *88*, 185–188.
7. Maeda, K., Kaji, R., Yasuno, K., Jambaldorj, J., Nodera, H., Takashima, H., Nakagawa, M., Makino, S., and Tamiya, G. (2007). Refinement of a locus for autosomal dominant hereditary motor and sensory neuropathy with proximal dominancy (HMSN-P) and genetic heterogeneity. J. Hum. Genet. *52*, 907–914.
8. Fukuda, Y., Nakahara, Y., Date, H., Takahashi, Y., Goto, J., Miyashita, A., Kuwano, R., Adachi, H., Nakamura, E., and Tsuji, S. (2009). SNP HiTLink: A high-throughput linkage analysis system employing dense SNP data. BMC Bioinformatics *10*, 121.
9. Gudbjartsson, D.F., Thorvaldsson, T., Kong, A., Gunnarsson, G., and Ingolfsdottir, A. (2005). Allegro version 2. Nat. Genet. *37*, 1015–1016.

10. Li, H., and Durbin, R. (2009). Fast and accurate short read alignment with Burrows-Wheeler transform. Bioinformatics *25*, 1754–1760.
11. Li, H., Handsaker, B., Wysoker, A., Fennell, T., Ruan, J., Homer, N., Marth, G., Abecasis, G., and Durbin, R.; 1000 Genome Project Data Processing Subgroup. (2009). The Sequence Alignment/Map format and SAMtools. Bioinformatics *25*, 2078–2079.
12. Robinson, J.T., Thorvaldsdóttir, H., Winckler, W., Guttman, M., Lander, E.S., Getz, G., and Mesirov, J.P. (2011). Integrative genomics viewer. Nat. Biotechnol. *29*, 24–26.
13. Neumann, M., Sampathu, D.M., Kwong, L.K., Truax, A.C., Micsenyi, M.C., Chou, T.T., Bruce, J., Schuck, T., Grossman, M., Clark, C.M., et al. (2006). Ubiquitinated TDP-43 in frontotemporal lobar degeneration and amyotrophic lateral sclerosis. Science *314*, 130–133.
14. Arai, T., Hasegawa, M., Akiyama, H., Ikeda, K., Nonaka, T., Mori, H., Mann, D., Tsuchiya, K., Yoshida, M., Hashizume, Y., and Oda, T. (2006). TDP-43 is a component of ubiquitin-positive tau-negative inclusions in frontotemporal lobar degeneration and amyotrophic lateral sclerosis. Biochem. Biophys. Res. Commun. *351*, 602–611.
15. Hasegawa, M., Arai, T., Nonaka, T., Kametani, F., Yoshida, M., Hashizume, Y., Beach, T.G., Buratti, E., Baralle, F., Morita, M., et al. (2008). Phosphorylated TDP-43 in frontotemporal lobar degeneration and amyotrophic lateral sclerosis. Ann. Neurol. *64*, 60–70.
16. Inukai, Y., Nonaka, T., Arai, T., Yoshida, M., Hashizume, Y., Beach, T.G., Buratti, E., Baralle, F.E., Akiyama, H., Hisanaga, S., and Hasegawa, M. (2008). Abnormal phosphorylation of Ser409/410 of TDP-43 in FTLD-U and ALS. FEBS Lett. *582*, 2899–2904.
17. Stieber, A., Chen, Y., Wei, S., Mourelatos, Z., Gonatas, J., Okamoto, K., and Gonatas, N.K. (1998). The fragmented neuronal Golgi apparatus in amyotrophic lateral sclerosis includes the trans-Golgi-network: Functional implications. Acta Neuropathol. *95*, 245–253.
18. Kuroda, Y., Sako, W., Goto, S., Sawada, T., Uchida, D., Izumi, Y., Takahashi, T., Kagawa, N., Matsumoto, M., Matsumoto, M., et al. (2012). Parkin interacts with Klokin1 for mitochondrial import and maintenance of membrane potential. Hum. Mol. Genet. *21*, 991–1003.
19. Greco, A., Mariani, C., Miranda, C., Lupas, A., Pagliardini, S., Pomati, M., and Pierotti, M.A. (1995). The DNA rearrangement that generates the TRK-T3 oncogene involves a novel gene on chromosome 3 whose product has a potential coiled-coil domain. Mol. Cell. Biol. *15*, 6118–6127.
20. Hernández, L., Pinyol, M., Hernández, S., Beà, S., Pulford, K., Rosenwald, A., Lamant, L., Falini, B., Ott, G., Mason, D.Y., et al. (1999). TRK-fused gene (TFG) is a new partner of ALK in anaplastic large cell lymphoma producing two structurally different TFG-ALK translocations. Blood *94*, 3265–3268.
21. Hisaoka, M., Ishida, T., Imamura, T., and Hashimoto, H. (2004). TFG is a novel fusion partner of NOR1 in extraskeletal myxoid chondrosarcoma. Genes Chromosomes Cancer *40*, 325–328.
22. Witte, K., Schuh, A.L., Hegermann, J., Sarkeshik, A., Mayers, J.R., Schwarze, K., Yates, J.R., 3rd, Eimer, S., and Audhya, A. (2011). TFG-1 function in protein secretion and oncogenesis. Nat. Cell Biol. *13*, 550–558.
23. Dion, P.A., Daoud, H., and Rouleau, G.A. (2009). Genetics of motor neuron disorders: New insights into pathogenic mechanisms. Nat. Rev. Genet. *10*, 769–782.
24. Andersen, P.M., and Al-Chalabi, A. (2011). Clinical genetics of amyotrophic lateral sclerosis: What do we really know? Nat Rev Neurol *7*, 603–615.
25. Ince, P.G., Highley, J.R., Kirby, J., Wharton, S.B., Takahashi, H., Strong, M.J., and Shaw, P.J. (2011). Molecular pathology and genetic advances in amyotrophic lateral sclerosis: an emerging molecular pathway and the significance of glial pathology. Acta Neuropathol. *122*, 657–671.
26. Cox, L.E., Ferraiuolo, L., Goodall, E.F., Heath, P.R., Higginbottom, A., Mortiboys, H., Hollinger, H.C., Hartley, J.A., Brockington, A., Burness, C.E., et al. (2010). Mutations in CHMP2B in lower motor neuron predominant amyotrophic lateral sclerosis (ALS). PLoS ONE *5*, e9872.
27. Tudor, E.L., Galtrey, C.M., Perkinton, M.S., Lau, K.-F., De Vos, K.J., Mitchell, J.C., Ackerley, S., Hortobágyi, T., Vámos, E., Leigh, P.N., et al. (2010). Amyotrophic lateral sclerosis mutant vesicle-associated membrane protein-associated protein-B transgenic mice develop TAR-DNA-binding protein-43 pathology. Neuroscience *167*, 774–785.
28. Lee, E.B., Lee, V.M., and Trojanowski, J.Q. (2012). Gains or losses: Molecular mechanisms of TDP43-mediated neurodegeneration. Nat. Rev. Neurosci. *13*, 38–50.
29. DeJesus-Hernandez, M., Mackenzie, I.R., Boeve, B.F., Boxer, A.L., Baker, M., Rutherford, N.J., Nicholson, A.M., Finch, N.A., Flynn, H., Adamson, J., et al. (2011). Expanded GGGGCC hexanucleotide repeat in noncoding region of C9ORF72 causes chromosome 9p-linked FTD and ALS. Neuron *72*, 245–256.
30. Renton, A.E., Majounie, E., Waite, A., Simón-Sánchez, J., Rollinson, S., Gibbs, J.R., Schymick, J.C., Laaksovirta, H., van Swieten, J.C., Myllykangas, L., et al; ITALSGEN Consortium. (2011). A hexanucleotide repeat expansion in C9ORF72 is the cause of chromosome 9p21-linked ALS-FTD. Neuron *72*, 257–268.